# CHAPTER 12

# Petrophysics of the Lance Sandstone Reservoirs in Jonah Field, Sublette County, Wyoming

SUZANNE G. CLUFF
The Discovery Group, Inc., Denver, Colorado, U.S.A.

ROBERT M. CLUFF
The Discovery Group, Inc., Denver, Colorado, U.S.A.

## ABSTRACT

Jonah field is a giant gas field producing from extremely low-porosity and low-permeability sandstones. Wire-line–log data from 62 wells near the center of the field were studied to characterize the porosity, permeability, and water saturation of the Lance reservoirs. The logs were environmentally corrected and normalized, shale volume and porosities were calculated, water saturations were determined by the dual water model, and net pay was calculated using field-specific pay criteria. Ultimate gas recovery per well was estimated by decline curve analysis of monthly production data.

Within the upper 2500 ft (760 m) of the Lance Formation, which includes the entire productive interval in nearly all wells, the average well has 1000 ft (30 m) of net sandstone, having an average porosity of 6.4%. The average permeability of all sandstones, estimated from core data-derived equations, is an astonishingly low 6 μd. The average water saturation of all sandstones is 45%.

Net pay criteria were determined from cumulative storage-capacity and cumulative flow-capacity plots. Although the average sandstone may have only 6% porosity, the low-porosity sandstones contribute an insignificant fraction of the reservoir flow capacity. We estimate that more than 95% of the flow capacity is from sandstones with greater than 6% porosity. A small percentage of high-porosity (>10%) and high-permeability rocks dominate the flow behavior of the reservoir and are probably critical to economic production. Using 6% porosity as an absolute net pay cutoff, the average net pay thickness at Jonah is 440 ft (130 m), with 9.3% porosity and 33% water saturation. The estimated average permeability of net pay is 25 μd. Estimated ultimate recovery per well is approximately 4 bcf gas on current 40-ac (0.16-km$^2$) well spacing.

## INTRODUCTION

Jonah field, located in Sublette County, Wyoming, was one of the largest onshore natural gas discoveries of the 1990s in the United States. Although many aspects of this field challenge our perceptions of what is required to form a giant gas accumulation, one of the most remarkable aspects are the petrophysics of the productive sandstones. The reservoir sandstones at Jonah have average porosities and permeabilities that would be considered the sealing facies in many gas fields, which immediately raises questions of how pay is defined and what constitutes valid criteria for differentiating pay from nonpay intervals.

The purpose of this chapter is to document the petrophysical properties of the Lance sandstones at Jonah

*Jonah Field: Case Study of a Giant Tight-Gas Fluvial Reservoir*, J. W. Robinson and K. W. Shanley, eds.: AAPG Studies in Geology 52 and Rocky Mountain Association of Geologists 2004 Guidebook

field, evaluate criteria for defining net pay, and propose a methodology to determine net pay cutoffs.

## METHODS

### Data Sources

Wire-line–log data from 62 wells near the center of Jonah field were selected for study out of a total of nearly 400 wells drilled by the end of 2002 (Figure 1). Although not every well in the field was included in the summations used for this chapter, we have run comparable calculations on many other wells across the field area and consider the wells in the central field area to be a representative sample for the productive Lance Formation. The data set includes several wells in the uppermost and the lowermost quartiles of the reserve size distribution of the field.

The basic analysis procedure we used involves the following steps, each of which is described in the following sections:

(1) Acquire data from either vendor field tapes or high-accuracy digitization of paper log prints;
(2) Merge log runs and depth shift curves between logging passes, if required;
(3) Import and depth shift core data;
(4) Apply environmental corrections and normalize porosity and gamma-ray logs;
(5) Compute shale volume from the gamma ray;
(6) Compute total porosity and shale-corrected ("effective") porosity from the density, neutron, and sonic logs;

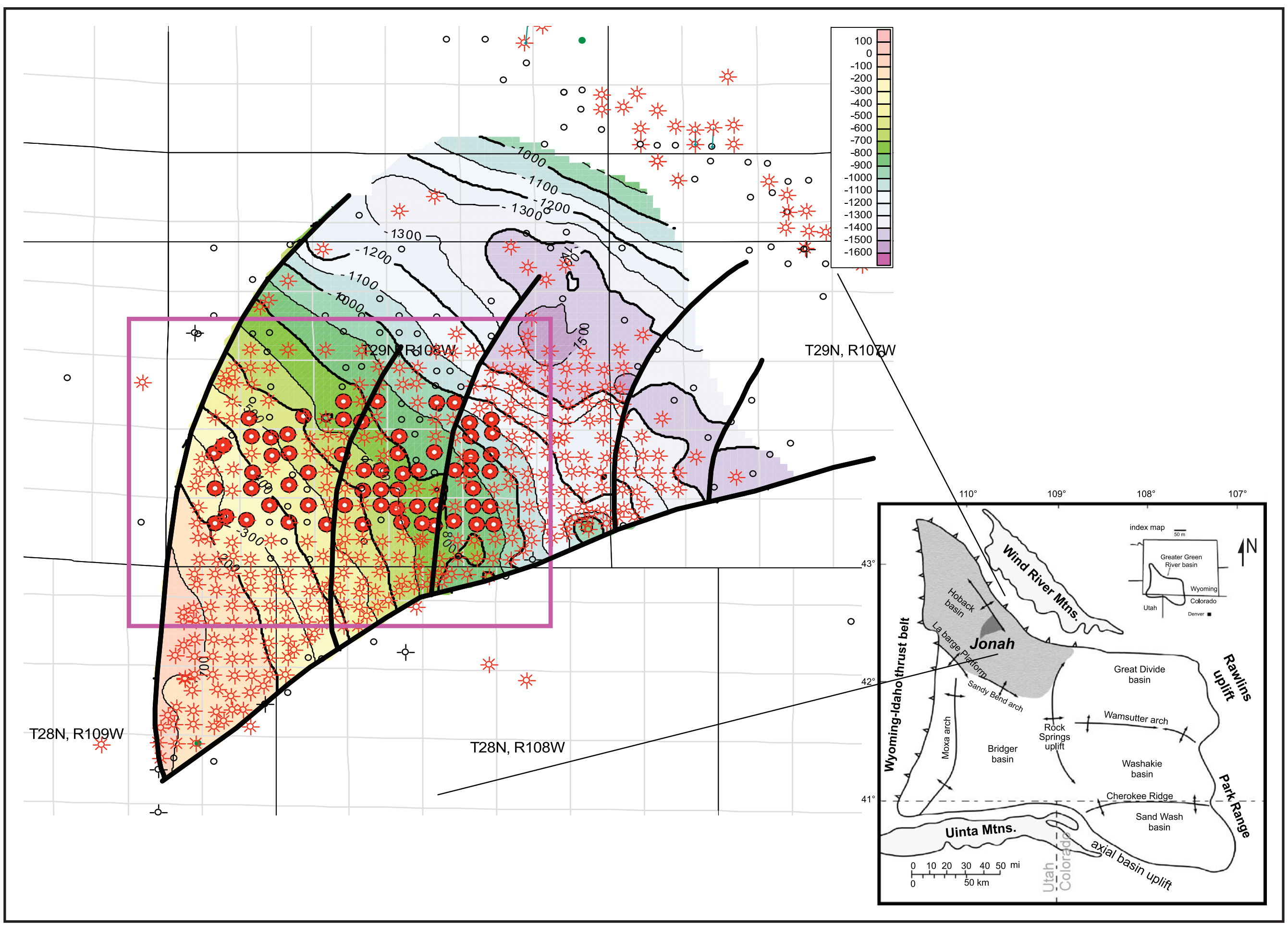


**Figure 1.** Structure contour map on the base of the Tertiary Fort Union Formation. Solid circles denote the location of wells used in the study. The study area is shown by the outline. Contour interval = 100 ft (30 m).

(7) Compute water saturation by dual water model;
(8) Calculate net pay using field-specific net pay cutoffs.

For this study, most of the logs were digitized from paper copies. Nearly all wells have been logged with an array induction resistivity tool and a compensated neutron-compensated density-gamma ray tool. Only a few sonic logs have been run in the field.

All logging run data were merged and depth shifted into alignment with the resistivity logs, which were assumed to be the reference depth in all cases. Because a large portion of the wells at Jonah were logged with a Schlumberger Platform Express tool, which includes the resistivity and porosity measurements all on a single tool string, relatively few wells require significant depth shifting.

Core data were available for four wells in the field, including porosity and permeability at net overburden stress conditions. The core data were imported as ASCII files, merged with the open-hole logs, then depth shifted into alignment with the logs by correlation with the gamma-ray and porosity curves. A total of 225 core sample points were used.

## Environmental Corrections and Log Normalization

Most petrophysical field studies begin by normalizing the log data to minimize differences caused by random logging errors and other noise in the data set. This noise results from a variety of causes. Logging tools built by different vendors can have different responses to identical formation conditions. The study wells were drilled between 1995 and 2002 and logged by several different wire-line companies. Different generations of logging tools and different processing algorithms were used, depending on the vendor and when the well was logged. Logging tool response is also strongly affected by borehole and mud conditions. Environmental correction routines are used to compensate for most of these environmental effects, but many of the key variables are poorly known or are not measured, and all environmental correction algorithms assume ideal, commonly unrealistic conditions (e.g., a perfectly centered tool in a cylindrical borehole). The environmental corrections applied to this data included (1) borehole size and mud weight correction to the gamma-ray logs; (2) matrix corrections to the neutron porosity; and (3) invasion (or "tornado chart") corrections to the three-curve induction resistivity logs. Array induction logs were not environmentally corrected, and the deepest array curve was used as an approximation of true formation resistivity. Other common environmental corrections applied by the logging vendor were determined to be negligible for the borehole sizes and logging conditions at Jonah field or are compensated for by the normalization procedure described below.

Normalization is a process used to reduce the residual errors by comparing the log response in a zone of known and constant properties with the expected response in that lithology. For example, a clean tight limestone or an anhydrite bed might have consistent density, neutron porosity, and sonic transit time over a broad area and would be expected to have the same log response in every well. In practice, the log responses differ, because the wells were logged with different tools, borehole conditions varied, the environmental corrections did not exactly match the actual conditions during logging, a tool might have been miscalibrated, or the logging operator simply made an error. The normalization procedure to reduce these errors involves either applying an offset (bulk shift) to the log curve or applying a gain correction between two known end points. In some cases, both adjustments will be made to the observed response to achieve the expected response in the constant property intervals. In all cases, we assume the log response is linear over the range of interest and can be approximated by a simple slope-intercept method.

Unfortunately, normalization in the Green River basin is problematic because there are no zones with uniform lithology over a large geographic area. Many log analysts use statistical techniques to reduce the variation between wells toward a field or area average, but most of these methods run the risk of eliminating actual geologic variation (signal) as opposed to random noise between logging jobs. As an alternative, we make the assumption that the minimum porosity over a field size area will be constant. We believe that this assumption is reasonable, because burial depth and time-temperature history are the major controls on porosity loss, whereas mineralogical variations are secondary and tend to be minor over the area of a field. Porosity variations are minor in the Lance Formation in the immediate vicinity of Jonah field. Because the average porosity of an interval varies with the sand to shale (or net/gross) ratio, we made no attempt to normalize the average properties of the logs; only the minimum observed porosity in clean sandstones and siltstones is used.

Neutron-porosity and bulk-density logs were normalized to match a suite of eight "type" logs. Composite histograms for each measurement were constructed from the data over the top 1000 ft (300 m) of the Lance Formation in these wells (Figures 2, 3). The extreme *X*-axis intercepts are not significant and may be caused by a few anomalous points in one well. The minimum porosity for normalization is picked on the steep right slope of the histogram, which, in the case of Figure 2, is near a cumulative frequency

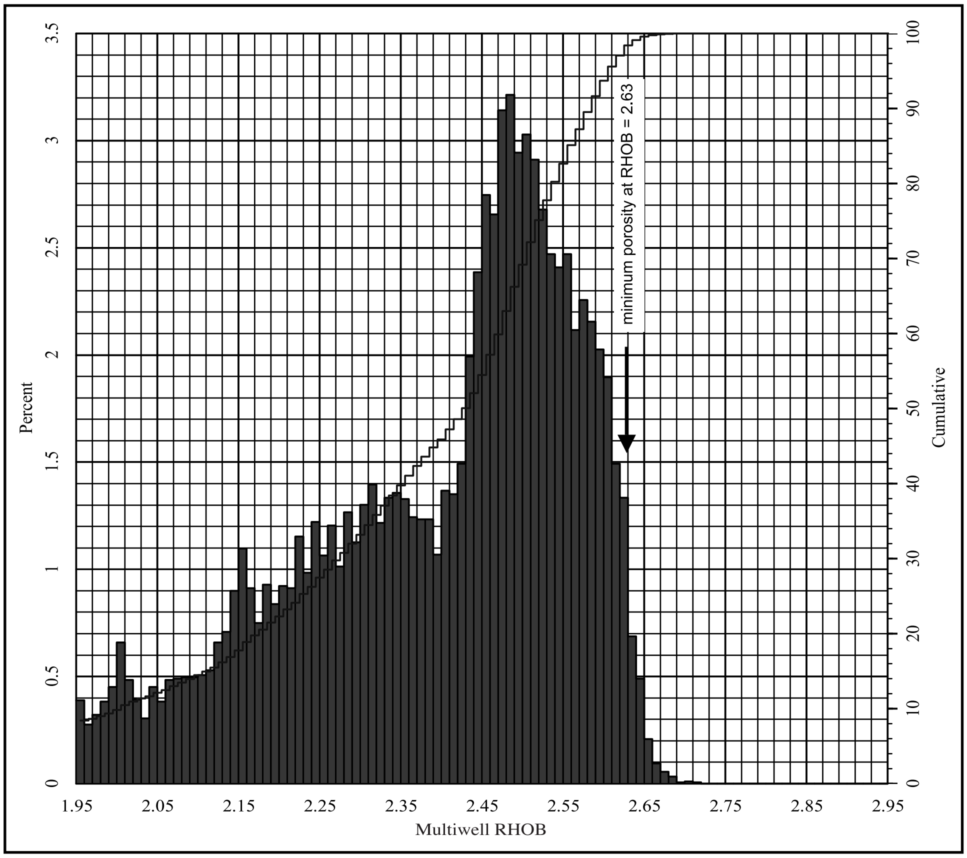


**Figure 2.** Type histogram for bulk-density (RHOB) log normalization. Histogram is a composite of the top 1000 ft (300 m) of the Lance Formation in eight wells. Histogram bars (frequency %) refer to left axis; cumulative frequency line (cumulative %) refers to the right axis.

of 98%. Minimum density porosity corresponds to tight siltstones with a bulk density of 2.63 g/cm$^3$ (1.5% porosity, Figure 2), and minimum neutron porosity in limestone units is 4.0% (Figure 3; equivalent to 7.5% on a sandstone matrix). Individual histograms of the equivalent stratigraphic interval in each well were then compared to the composite histograms to determine the normalization shift. Neutron logs show significant variation between vendors and from borehole environment effects. The differences are caused by temperature effects and variations in tool standoff. Density logs show only minor differences, on the order of ±0.02 g/cm$^3$, and are related to tool calibration and problems with the mud cake and borehole rugosity corrections. Because very few sonic logs were available in the study area, they were not used in the porosity analysis.

Gamma-ray logs are also normalized and require a two-point calibration procedure. A very significant and systematic difference in tool response was observed between logging vendors; we found that the published environmental correction routines only make a small reduction to these differences. In particular, two of the logging vendors in the Jonah-Pinedale area have similar tool response in the Lance Formation (after environmental corrections are applied), but one vendor reads consistently lower API values in both sandstones and shales. Reducing this variability by normalizing the gamma-ray logs greatly simplifies correlation and saturation calculations. Normalized gamma-ray logs are also essential for advanced formation evaluation methods, such as neural network modeling.

Gamma-ray logs were offset to match a consistent clean sandstone line, and a gain correction was applied to match the sandstone-to-shale span of the composite histogram in the same 8 wells used for the porosity normalization (Figure 4). The form of the equation used was

$$\mathrm{GRC} = [(\mathrm{GR} - \mathrm{GRsd}) \times (\mathrm{GRsh\_T} - \mathrm{GRcl\_T})/ (\mathrm{GRsh} - \mathrm{GRsd})] + \mathrm{GRcl\_T} \qquad (1)$$

where GR is the environmentally corrected log value at each depth, GRcl_T is the target clean sandstone value from the type histogram (45 API units), GRsh_T is the target shale value from the type histogram (110 API units), GRsd is the observed sandstone reading on the subject well histogram, and GRsh is the observed shale reading on the subject well histogram. It should be emphasized that the choice of target values is somewhat

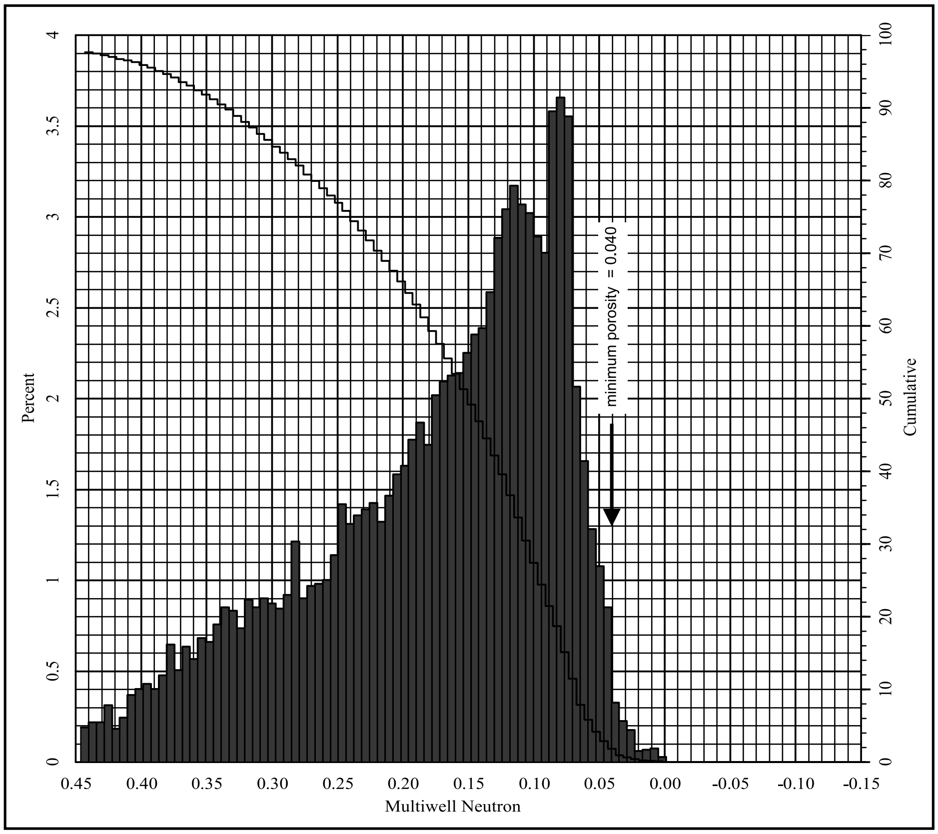


**Figure 3.** Type histogram for neutron-porosity normalization. Histogram is a composite of the top 1000 ft (300 m) of the Lance Formation in eight wells. Porosity was converted from field logging units (sandstone) to limestone units for this analysis. Histogram bars (frequency %) refer to left axis; cumulative frequency line (cumulative %) refers to the right axis.

arbitrary. The values selected should be distinctive features on the type histogram for which corresponding points can easily be recognized on histograms of individual logs in the area.

As a check of the normalization assumptions, the bulk shifts are mapped to see if variations form a random pattern (noise) or any kind of organized geographic distribution. If the latter is true, the assumption is that the variations are related to geology instead of logging tool response, calibration, or the borehole environment. At Jonah field, all of the normalization corrections appear either random or vendor related in most wells. With the exception of gamma-ray log shifts the corrections were relatively small.

## Shale Volume, Total Porosity, and Effective Porosity

Volume of shale ($V_{\text{shale}}$) was computed from the gamma-ray curve with a simple linear $V_{\text{shale}}$ equation:

$$V_{\text{shale}} = (\text{GRC} - \text{GRsd})/(\text{GRsh} - \text{GRsd}) \quad (2)$$

where GRC is the environmentally corrected and normalized gamma ray from equation 1, GRsd is the normalized value for clean sandstone (45 API units), and GRsh is the normalized value for shale (110 API units).

"Total porosity" is the total pore volume of the rock and includes porosity filled with hydrocarbons, moveable water, capillary-bound water, and clay-bound water (Hook, 2003). Both the density and neutron logs are considered total porosity tools, because they detect all the porosity in a region surrounding the logging tool, although they have different volumes of investigation and are responding to different physical phenomena that are indirectly related to porosity (electron density in the case of the bulk-density log and hydrogen density in the case of the neutron log). In shaly formations, they read very different values; in particular, the neutron log is strongly affected by hydrogen associated with clay-bound water and reads a much higher apparent porosity than the density log. "Effective porosity" is normally considered that part of the total porosity that is available for hydrocarbon storage and is also physically interconnected so that fluids can actually move between the pores. In vuggy carbonate rocks, for example, there may be isolated vugs that are part of the total porosity, but which have no pore throats that would allow fluids to move in or out of the vugs. These are not considered part of the effective pore system. In shaly sandstones, a

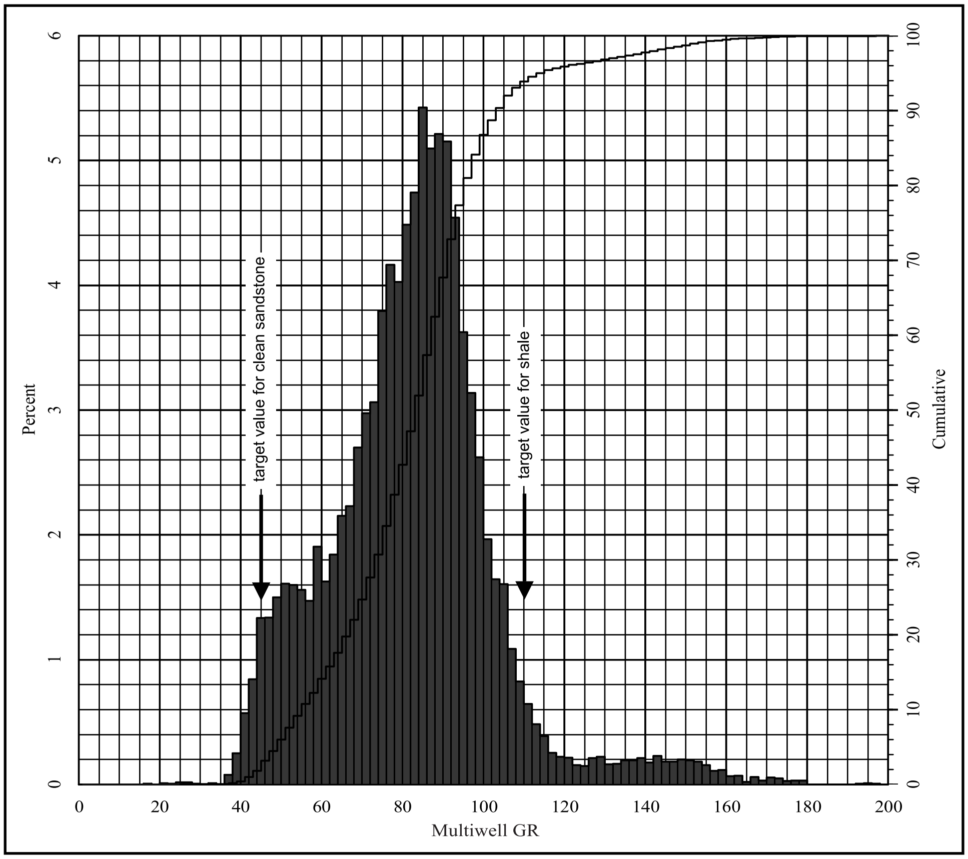


**Figure 4.** Type histogram for gamma-ray (GR) log normalization. Histogram is a composite of the top 1000 ft (300 m) of the Lance Formation in eight wells. Arbitrary target values for clean sandstone and shale are marked. Histogram bars (frequency %) refer to left axis; cumulative frequency line (cumulative %) refers to the right axis.

significant portion of the porosity is occupied by clay-bound water that is immobile under all conditions and consequently is not part of the effective pore space. We use effective porosity for the fraction of the total porosity that is not associated with clay minerals, thus excluding the volume of clay-bound water but including capillary-bound water on grain surfaces. By this definition, the effective porosity of shale is zero, whereas a clean sandstone has an effective porosity equal to the total porosity. Because it is unlikely that there is much truly isolated porosity in fine-grained clastic rocks, this definition of effective porosity is very close to the hydraulically connected pore volume. Our definition of effective porosity in shaly sandstones is the same as that used in several log analysis textbooks (e.g., Dewan, 1983; Asquith, 1990).

Total porosity was calculated from the normalized density and neutron logs using the appropriate (vendor-specific) crossplot. Total density porosity was calculated using 2.65 g/cm$^3$ grain density. The neutron porosity was converted from field-reported units (sandstone matrix) to limestone units prior to normalization and analysis. Most advanced log interpretation routines, including all crossplot porosity charts, require the neutron log to be in limestone units.

Effective porosity was computed separately for each porosity tool from the matrix-corrected total porosity, $V_{\mathrm{shale}}$, and average values for the total porosity of shale by equations of the form

$$\mathrm{PHIDE} = \mathrm{PHID} - (V_{\mathrm{shale}} \times \mathrm{PHID}_{\mathrm{shale}}) \tag{3}$$

where PHIDE is the effective porosity from the density log, PHID is the total porosity from the density log, $\mathrm{PHID}_{\mathrm{shale}}$ is the total density porosity of shale, and $V_{\mathrm{shale}}$ is the linear shale index from equation 2. Analogous equations were used to compute effective neutron porosity and effective sonic porosity. The average values for the total porosity of shale in these equations were 2.4% density porosity, 24% neutron porosity (sandstone matrix), and 21% sonic porosity. The calculated sum-of-squares average of the effective density and neutron porosities closely approximates a gas effect-corrected effective porosity. This value was used in all subsequent calculations and reservoir property summations.

The calculated effective porosity matches the overburden-corrected core porosity and is slightly less than the average field-measured density porosity, as would be expected if gas is present in the formation. Although routine core porosity is generally considered a total porosity measurement, it is only true if the core plugs are dried at high temperature and all clay-bound water is driven off. Many operators use density porosity as an approximation of effective porosity. This work confirmed that this is a reasonable quick-look method because the bulk density of compacted shale in the Lance is fairly close to the matrix density of sandstone. Because the density log can indicate too high a porosity in gas-bearing sandstones, the shale-corrected density-neutron effective porosity is a more accurate measure of pore volume available for hydrocarbon storage.

### Water Saturation

Water saturations were computed using the dual water model (Clavier et al., 1977), with a constant $R_{\mathrm{wf}}$ (formation water resistivity) at formation temperature of 0.18 ohm m and an $R_{\mathrm{wb}}$ (bound water resistivity) of 0.20 ohm m. These values were derived from Pickett plots and crossplots of apparent water resistivity versus shale volume. Because $R_{\mathrm{wf}}$ and $R_{\mathrm{wb}}$ are similar, the clay conductivity correction is minor, and the results are similar to a simple Archie saturation calculation. The cementation exponent ($m$) and saturation exponent ($n$) were both set to 1.8 based on crossplots and our general knowledge of pore structure in tight-gas sandstones.

Substantial uncertainty is associated with both water resistivity estimates and electrical exponents. Produced water in the field is limited (average 3.1 bbl/mmcf gas), and it contains mud filtrate, completion fluids, and water of condensation from the gas stream. The $R_{\mathrm{wb}}$ estimate is generally consistent with the clay mineralogy of the Lance and is reasonably constrained from the log data. It is likely that $R_{\mathrm{wf}}$ varies through the Lance and across the field area as a function of variation in formation temperature and depth. Unfortunately, data are insufficient to determine the $R_{\mathrm{w}}$ gradient or zonation, so a constant $R_{\mathrm{w}}$ was used, which yields a simplified but easily reproducible set of calculations. The $m$ and $n$ exponents can be determined by special core analysis methods, but these data have not been released by any of the operators at Jonah field.

### Estimated Ultimate Recovery

Estimated ultimate recovery (EUR) was determined by conventional decline curve analysis of the production histories through mid-2001 (Cluff, 2004, Appendix C). The production data were obtained from a commercial vendor. Preliminary estimates of the initial decline rates and hyperbolic decline exponents were based on the older wells in the field. A hyperbolic exponent ($b$) of 0.85 matched the curvature of the decline curve in most wells. Initial decline rates vary but average 70%. Recently, drilled wells with insufficient production history were compared with offset wells to estimate the decline rate and curvature. Decline rates were not limited to a constant exponential rate at the tail of the curve. All wells were projected to a constant economic rate limit ($Q_{\mathrm{ec}}$) of 2 mmcf gas/month. Using a constant rate limit eliminates pricing and operating cost assumptions.

## PETROPHYSICS OF THE LANCE FORMATION

Because wells in Jonah field were drilled to different total depths and few wells penetrate the entire Lance Formation, it is difficult to sum the petrophysical properties in a manner that allows meaningful well-to-well comparisons without the thickness of section drilled becoming a significant variable. No reliable stratigraphic markers in the Lance section, particularly in the lower Lance, allow us to subdivide the formation into zones that a majority of geologists would agree are correlative depositional units. As a compromise, we summed the petrophysical properties of the top 2500 ft (760 m) of the formation. The top of the interval is the base of the Tertiary Fort Union Formation (Tfu0 horizon; Cluff and Murphy, 2004), which is a more consistent and reliable correlation surface than the top of the Lance Formation. The top of the Lance can be picked at different positions within or below a 200–500-ft (60–150-m) shaly unit (averages 325 ft [100 m]), informally called the "Unnamed Tertiary shale" by several operators or the "Not Yet" by local mud-loggers (DuBois et al., 2004; Cluff and Murphy, 2004, Appendix B). Palynological data collected by Chevron U.S.A. (unpublished data shown by Bowker and Robinson, 1997) suggest that the Cretaceous–Tertiary boundary lies somewhere in the Unnamed shale section. All the wells in the study area penetrate the entire 2500-ft (760-m) interval below the base of the Fort Union. It should be noted that the upper 2500 ft (760 m) of the Lance Formation in this study includes the abovementioned Unnamed shale unit.

### Net Sandstone Thickness

Net sandstone is defined as having less than 50% $V_{\mathrm{shale}}$ using the linear gamma-ray index method described above. Ignoring the previously discussed vendor variability and borehole effects, the 50% $V_{\mathrm{shale}}$ cutoff roughly corresponds to 75 API units, which is a commonly used field definition for sandstone.

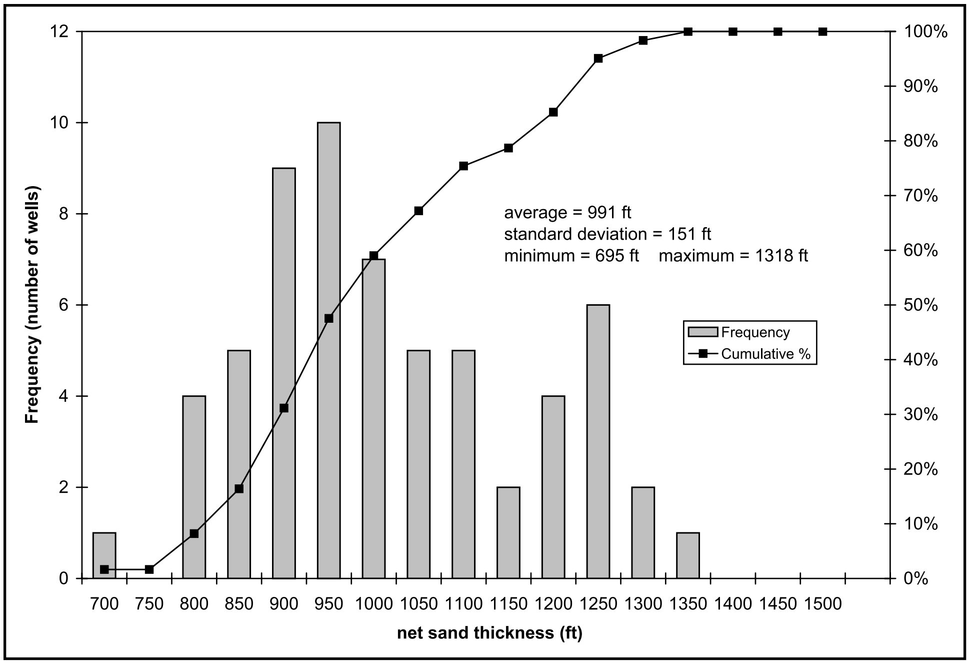


**Figure 5.** Distribution of total net sandstone thickness, by well, in the upper 2500 ft (760 m) of the Lance Formation. No porosity or water saturation cutoffs are applied. Histogram bars refer to left (frequency) axis; cumulative frequency line (cumulative %) refers to the right axis.

The net thickness of sandstone in the top 2500 ft (760 m) of the Lance ranges from 700 to 1300 ft (210 to 400 m) and averages a little less than 1000 ft (300 m) (Figure 5). The net/gross ratio ranges from 28 to 53% and averages 40% (Figure 6). Figures 7 and 8 show the areal distribution of these two parameters.

## Porosity

The average porosity determined from the available core data at Jonah field ($n$ = 225) is 7.7% (Figure 9). These core data are routine analyses at 800 psi confining stress and have not been corrected to net overburden

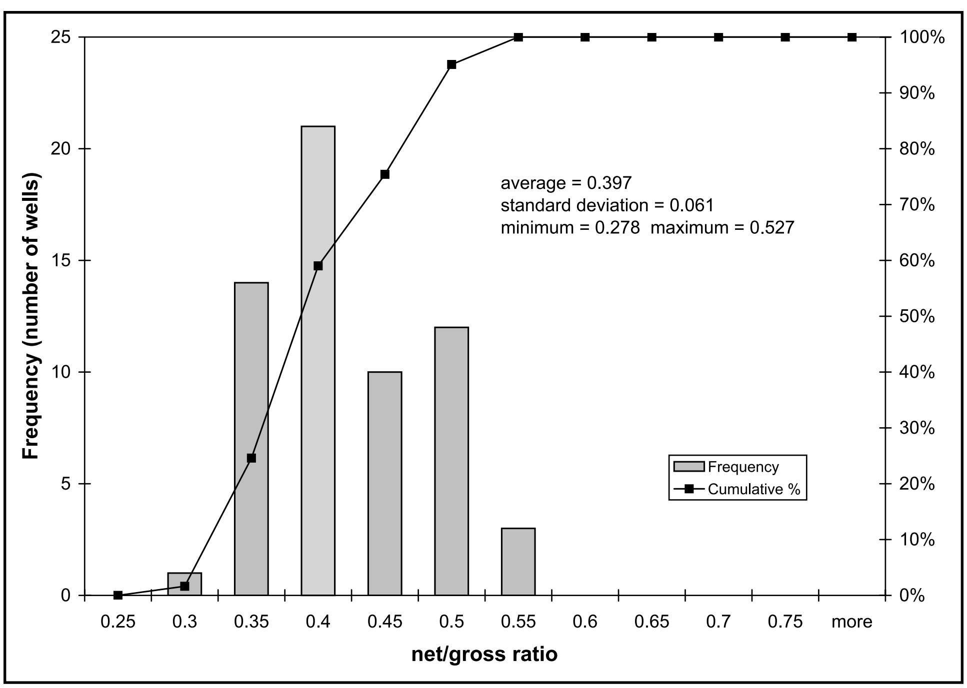


**Figure 6.** Distribution of the ratio of net sandstone to gross interval, by well, for the upper 2500 ft (760 m) of the Lance Formation. Histogram bars refer to left (frequency) axis; cumulative frequency line (cumulative %) refers to the right axis.

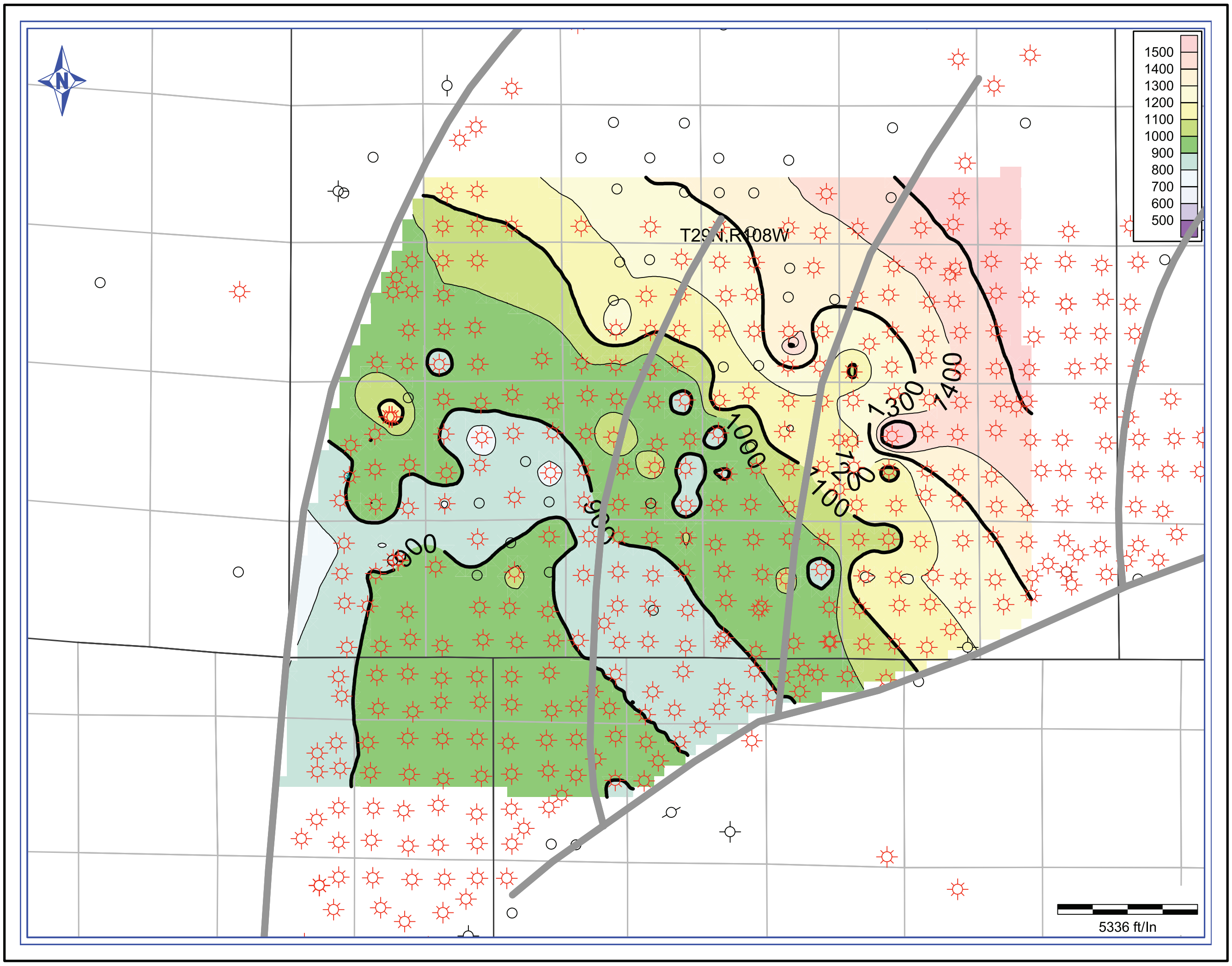


**Figure 7.** Net feet of sandstone in the upper 2500 ft (760 m) of the Lance Formation. Contour interval = 100 ft (30 m).

conditions. The correction from laboratory conditions to 4000 psi net effective overburden stress is given by the regression equation

$$\phi_{\text{in situ}} = 1.0077\ \phi_{\text{routine}} - 0.6482, \quad r^2 = 0.986 \tag{4}$$

where porosity is in percent (Figure 10). By this equation, the average routine core porosity of 7.7% is equivalent to an in-situ porosity of 7.1%.

The average log-determined porosity from all wells ranges from 4 to 10%, with an average of 6.5% (Figure 11). The difference between the average log porosity and average in-situ core porosity is not significant given the small sample size of the core data compared to the log data; furthermore, core plugs are commonly selected in a manner that undersamples the lowest porosity sandstones and siltstones. Figure 12 shows the essentially random variation in average porosity over the study area. Most wells exhibit a greater range of porosity values than the range of averaged porosities shown in Figures 11 and 12. This is illustrated by the well shown in Figure 13, which has a typical average porosity of 7.4%, but the total range of porosity is from 0 to 15%.

### Permeability

The average routine core permeability (800-psi net confining stress) is 145 μd (0.145 md) (Figure 14). In tight-gas sandstones, most reservoir units have average permeabilities less than 100 μd (0.1 md). To avoid the repetitive use of very small decimal fractions, we encourage using microdarcys (μd), where 1 μd = 0.001 md = $10^{-6}$ darcys.

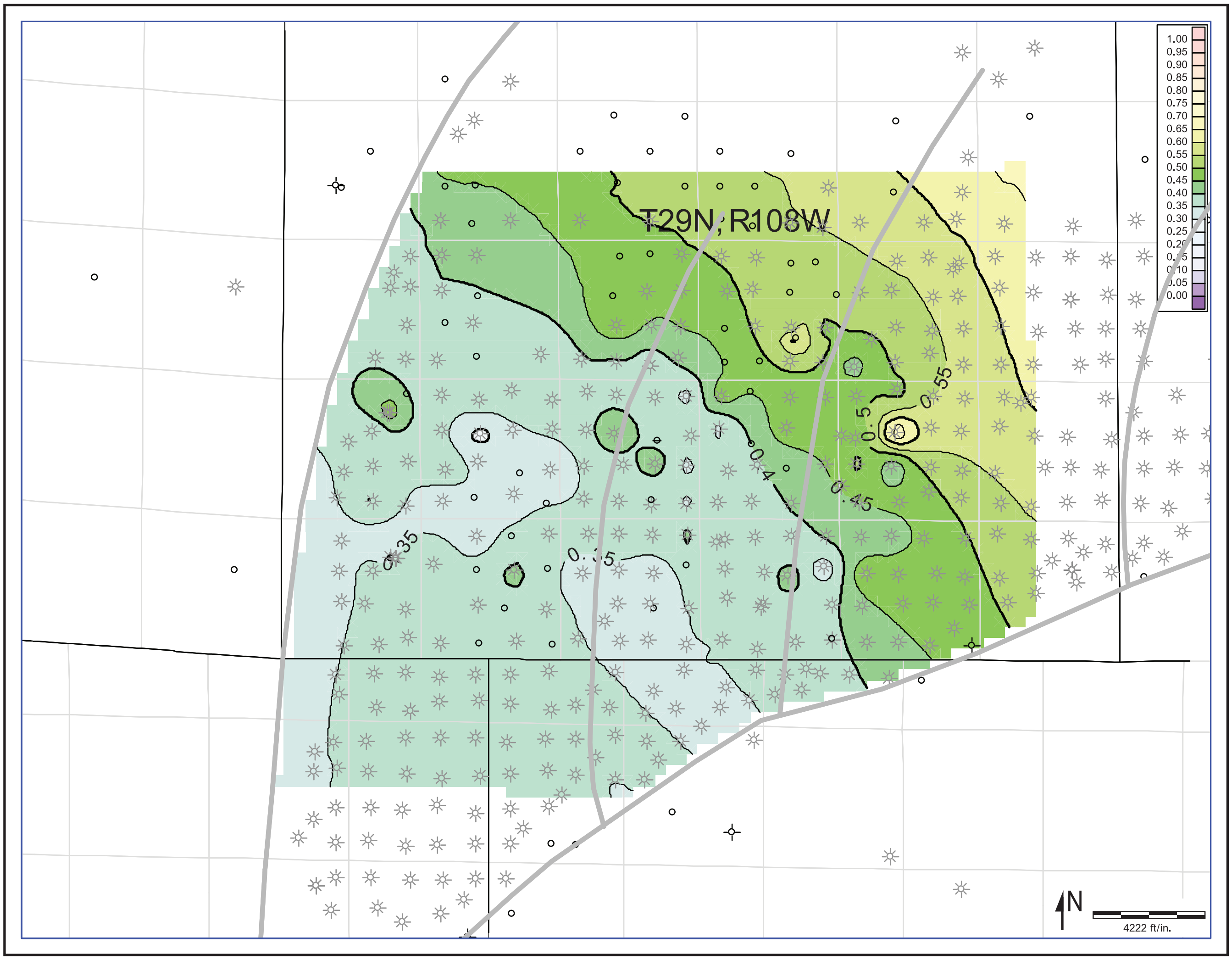


**Figure 8.** Ratio of net sand to gross interval in the upper 2500 ft (762 m) of the Lance Formation. Contour interval = 0.05%.

On the text figures and in equations that span to higher permeability values, we revert to the more conventional units of millidarcys.

Samples with the highest permeability are suspected to be microfractured plugs. Correction from ambient laboratory conditions to net overburden stress will reduce these values by at least 50%, and correction to effective permeability to gas at reservoir saturation will reduce them still further. Well performance data suggest that the average effective permeability to gas in typical Jonah wells are in the low tens of microdarcys (Eberhard and Mullen, 2001).

The correction from routine core analysis ($P$ = 800 psi) to Klinkenberg corrected permeability at net effective overburden stress ($P$ = 4000 psi) was determined by regression analysis of a subset of the core data ($n$ = 225) with several outliers removed:

$$\log_{10} K_{\infty\ 4000\ \text{psi}} = 1.4718 \times \log_{10}(K_{\text{air}\ 800\ \text{psi}}) - 0.4016, \quad r^2 = 0.922 \tag{5}$$

where permeability in this equation is in millidarcys (Figure 15). Using this equation, the average routine permeability of 145 μd is equivalent to an in-situ reservoir permeability of only 23 μd, or 16% of the routine analysis. This in-situ permeability is the average single-phase (or absolute) gas permeability at 0% water saturation and will be further reduced by the effects of relative permeability, unless the reservoir sandstones are at irreducible water saturation.

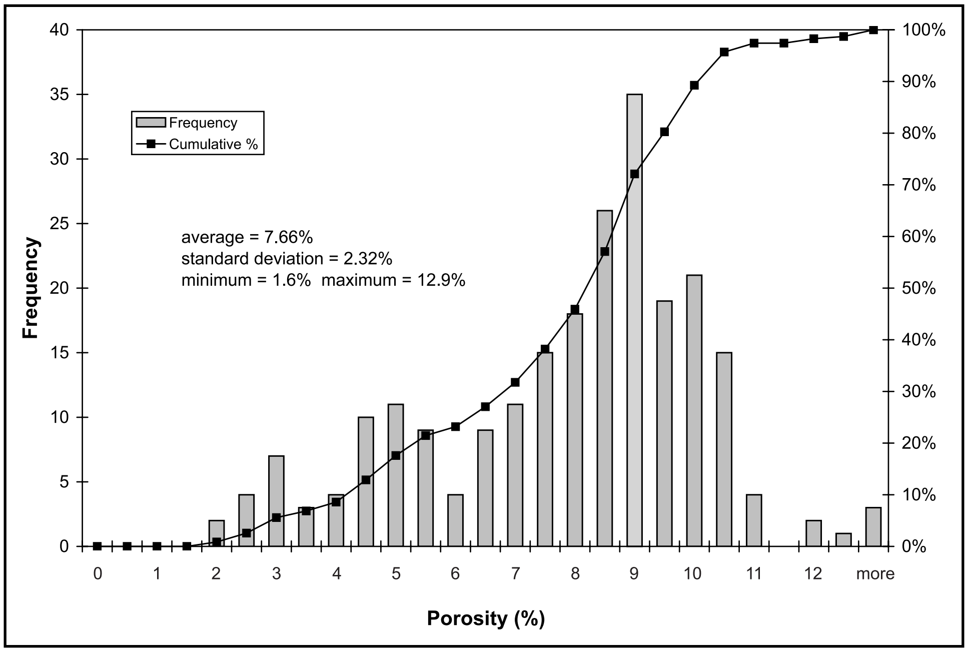


**Figure 9.** Distribution of routine core porosity values for the Lance Formation. Histogram bars refer to left (frequency) axis; cumulative frequency line (cumulative %) refers to the right axis.

The regression equations to estimate permeability from porosity (and vice versa) at reservoir stress condition are

$$\log_{10} K_{\infty\ 4000\ \mathrm{psi}} = 0.2135 \times \phi - 3.5861, \quad r^2 = 0.488 \tag{5.1}$$

$$\phi = 4.6838 \times (\log_{10} K_{\infty\ 4000\ \mathrm{psi}} + 3.5861) \tag{5.2}$$

where porosity is in percent, and permeability is in millidarcys (Figure 16). The poor correlation coefficient is typical of tight-gas sandstones. Equation 5.1 accurately expresses the average trend of increasing permeability with increasing porosity, but the scatter around the trend line is so great that the equation should be used with caution for quantitative prediction of flow capacity from porosity.

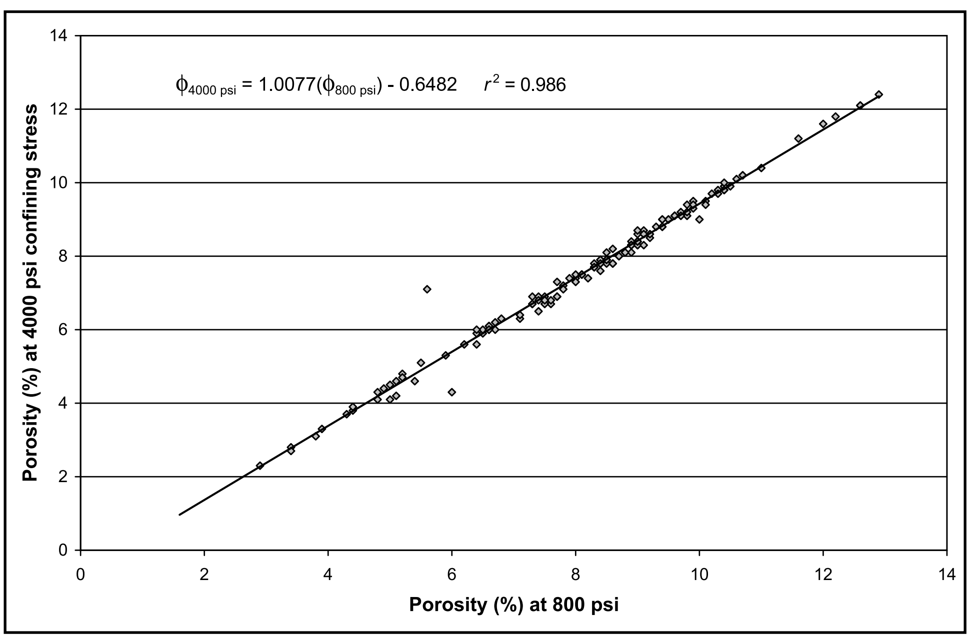


**Figure 10.** Correlation of routine core porosity (800 psi confining stress) and porosity at net overburden conditions (4000 psi confining stress).

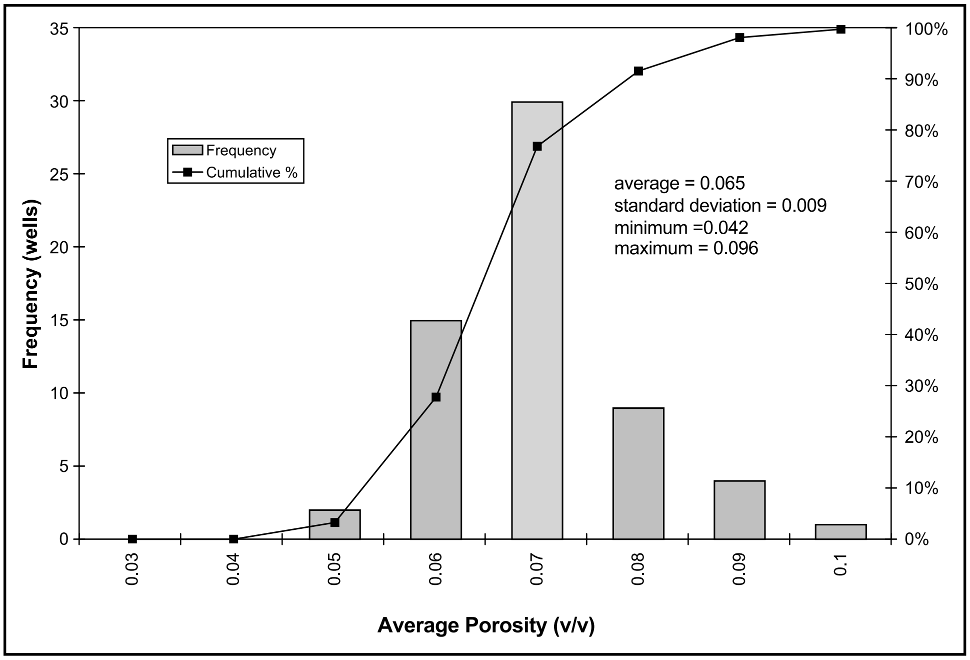


**Figure 11.** Distribution of average porosity, by well, in the upper 2500 ft (760 m) of the Lance Formation. Histogram bars refer to left (frequency) axis; cumulative frequency line (cumulative %) refers to the right axis.

### Water Saturation

The water saturation per well by log analysis ranged from 30 to 57%, with an average of 45% (Figure 17). Eberhard and Mullen (2001) reported a similar range of water saturations (30–60%). Water saturation correlates with porosity. Lower average water saturations in higher porosity rocks are observed in the log calculations and in routine core analyses (Figure 18). The product of water saturation and porosity (bulk volume water) is nearly constant at 3 to 3.5%, which suggests that the sandstones in Jonah field are near irreducible water saturation conditions. This observation is consistent with the very low produced water/gas ratio (WGR) in the updip wells.

No oil-based cores have been cut as of mid-2003 that would be useful for testing the validity of these values. Our calculated water saturations in cored intervals are similar to reported routine core saturations in magnitude and variation. The values are reasonable based on our knowledge of capillary-pressure characteristics of similar tight-gas sandstone reservoirs in the Rocky Mountain region (e.g., Byrnes, 1997). Bowker (1995) published a gas-brine capillary-pressure curve for one sample (9781 ft [2983 m], 9.7% porosity) from the Lance in the Jonah Federal 2-5 (Sec. 5, T28N, R108W). The curve never attains an asymptotic irreducible water saturation but climbs steeply between 35 and 20% water saturation at capillary pressures equivalent to 500–2000 ft (150–610 m) of gas above a free-water level. Because the gas accumulation at Jonah is at least 2500 ft (760 m) thick and, based on pressure data, appears to act like a common pool with one pressure gradient, it is reasonable to assume that the actual saturations attained in the field will be in this range. An attempt was made to discern a trend of increasing water saturation with depth from the well-log calculations but we were unable to define a meaningful saturation-height function given the uncertainty in the $R_w$ gradient across the field. A map of average water saturation of the Lance (Figure 19) does not show any meaningful pattern in average saturation. A map of water saturation (not included) filtered to the high-porosity rocks shows a very gradual and erratic decrease in water saturation updip toward the southwest corner of the field.

## NET PAY DETERMINATION

One of the most vexing problems in tight-gas sandstone formation evaluation is the determination of net pay. Engineers and petrophysicists have never settled on a rigorous definition for net pay, much less a standard methodology to decide what is or is not pay.

In a high porosity-permeability conventional hydrocarbon accumulation, net pay is defined on flow-rate criteria and the fluids produced. Rocks with sufficient permeability to flow fluids at commercially significant rates are classified as "net sandstone" or net reservoir. If

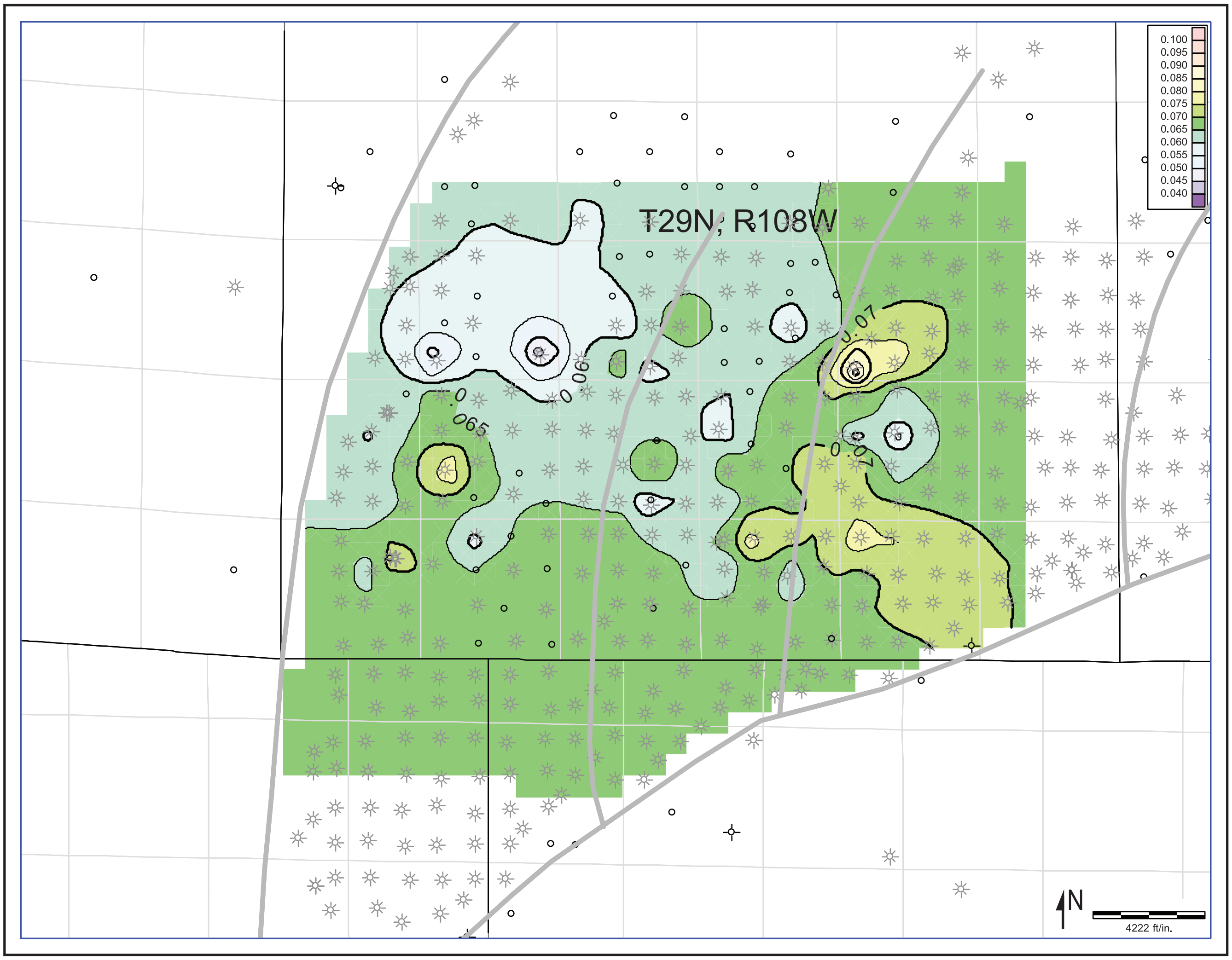


**Figure 12.** Contour map of average sandstone porosity in the upper 2500 ft (760 m) of the Lance Formation. Contour interval = 0.05%.

they produce hydrocarbons at a commercially acceptable hydrocarbon/water ratio, they are classified as net pay. Note the emphasis on commerciality in both cases; the word pay implies money and some kind of economic criteria. Also note that the petrophysical criteria most useful to distinguish pay from nonpay would be permeability, hydrocarbon saturation, and relative permeability to the hydrocarbon and water phases as a function of saturation. Only one of these factors (saturation) is routinely estimated from logging measurements.

This conventional notion of net pay leads to the common use of three log- or core-based petrophysical cutoffs to separate pay from nonpay:

(1) *Shaliness*: A volume of shale cutoff, commonly a gamma-ray or spontaneous potential cutoff, is used to separate potentially permeable clean formation from presumably impermeable shaly formation.

(2) *Porosity*: A porosity cutoff is used as a proxy for a permeability or flow cutoff. A porosity-permeability crossplot can be used to define a porosity equivalent to a minimum permeability considered capable of flowing hydrocarbons at commercial rates. Alternatively, a comparison of production test or drill-stem test flow rates on a large number of zones can be used to determine the minimum porosity required for a commercial completion.

(3) *Water saturation*: A calculated water saturation cutoff is used to separate wet zones from oil-bearing or gas-bearing pay intervals. In high-porosity and high-permeability sandstones, the transition zone from water wet to hydrocarbon saturation is commonly

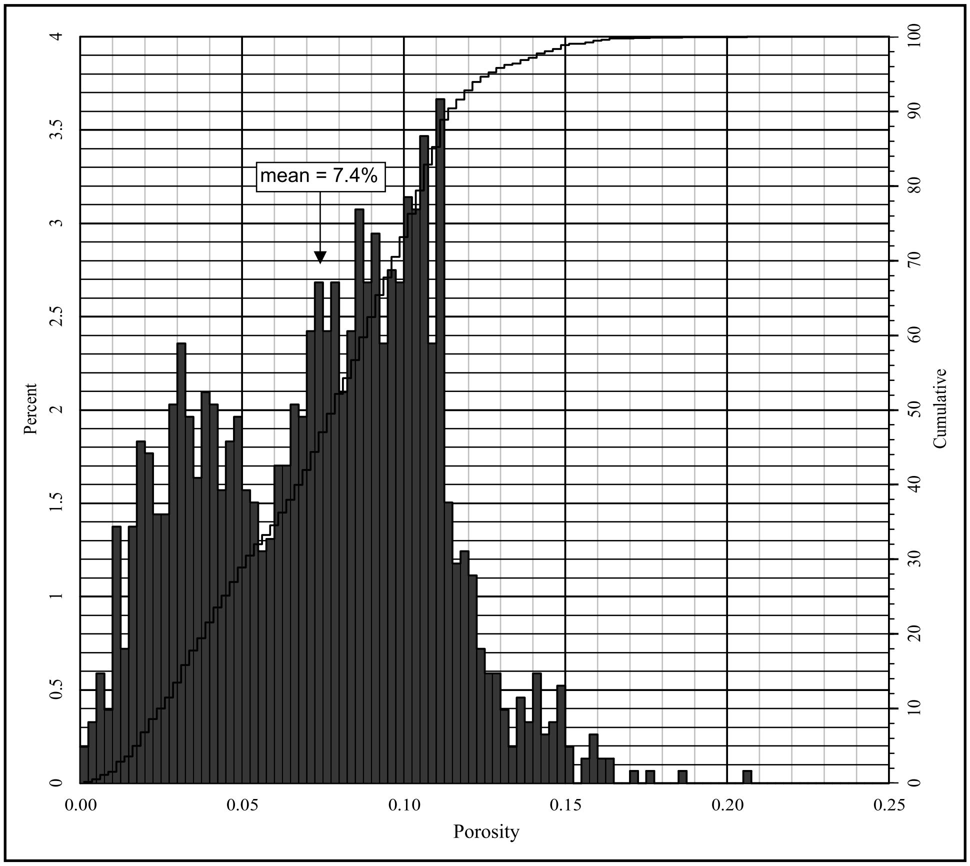


**Figure 13.** Sandstone porosity distribution for the upper 2500 ft (760 m) of the Lance Formation in a typical well near the center of Jonah field. Data samples greater than 12% porosity are bad log readings immediately adjacent to washed-out shale intervals. Histogram bars (frequency %) refer to left axis; cumulative frequency line (cumulative %) refers to the right axis.

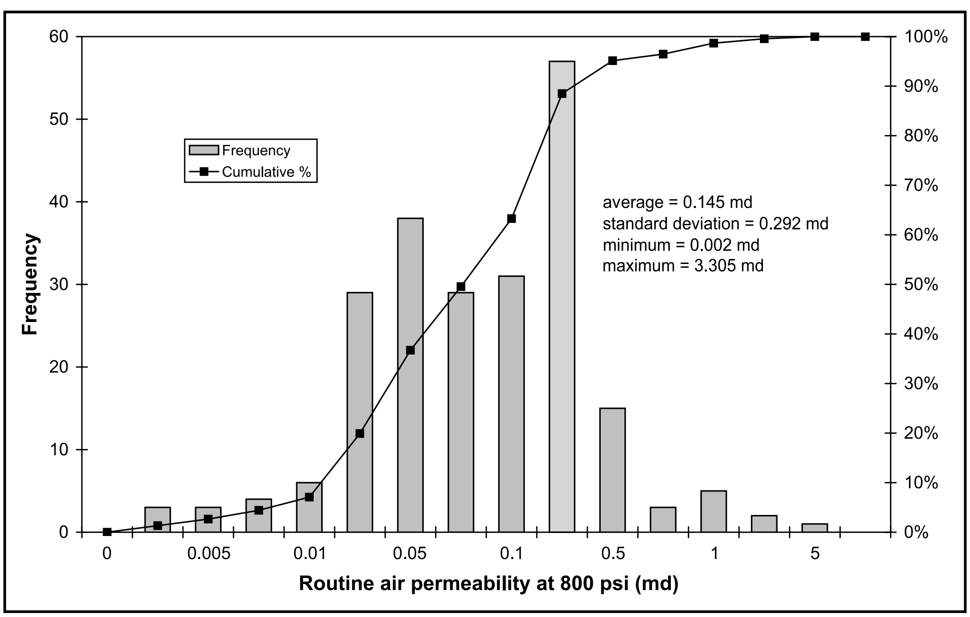


**Figure 14.** Distribution of routine core permeability values in the Lance Formation. Histogram bars refer to left (frequency) axis; cumulative frequency line (cumulative %) refers to the right axis.

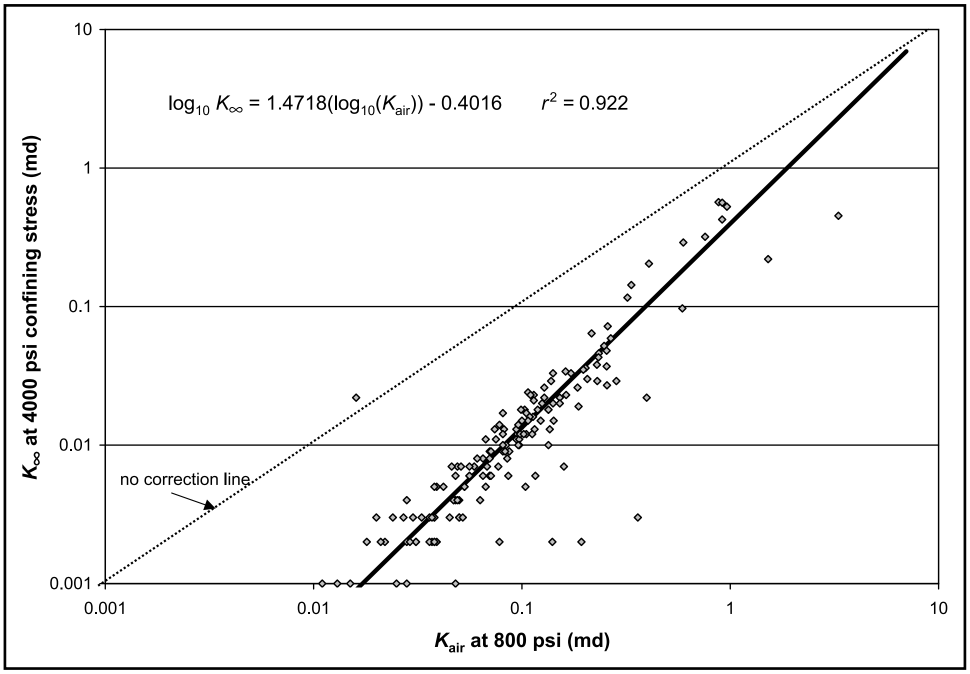


**Figure 15.** Correction from routine core permeability measurements to Klinkenberg corrected permeability at 4000 psi net confining stress.

very thin, with a significant difference in water saturation between high water saturation wet zones and low water saturation pay zones. Thus, the actual water saturation cutoff may not be critical, as long as it is between the average wet saturation and the typical hydrocarbon saturation.

In tight-gas sandstones, all of the above criteria become fuzzy, and decisions concerning net pay cutoffs have a significant impact on the net pay calculations. This affects both completion decisions and reserve calculations. Tight-gas sandstones include a shaly sand component, and the relationship between shaliness and permeability

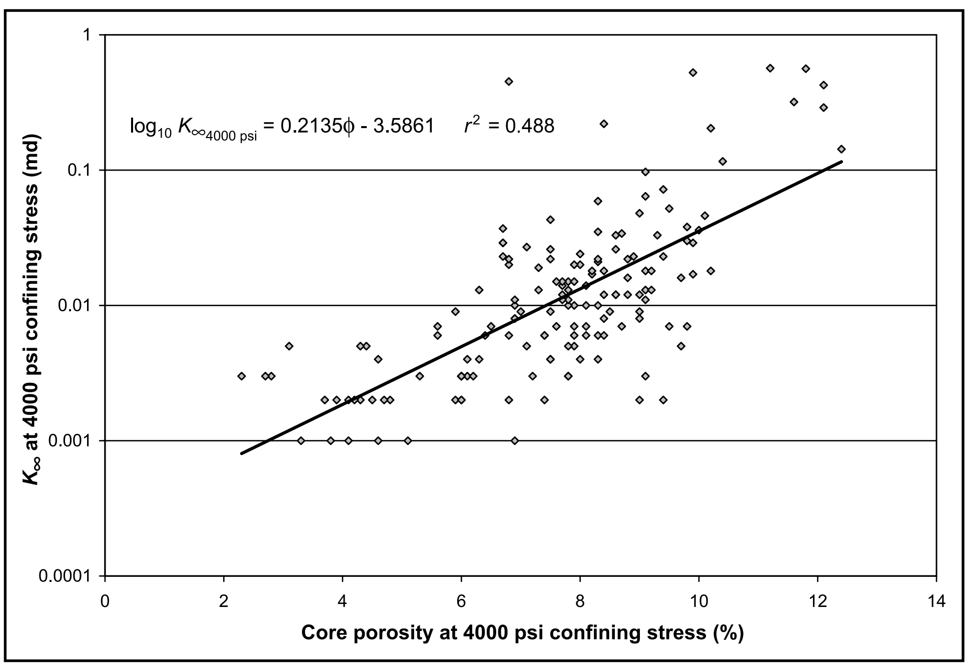


**Figure 16.** In-situ porosity to in-situ Klinkenberg corrected permeability correlation.

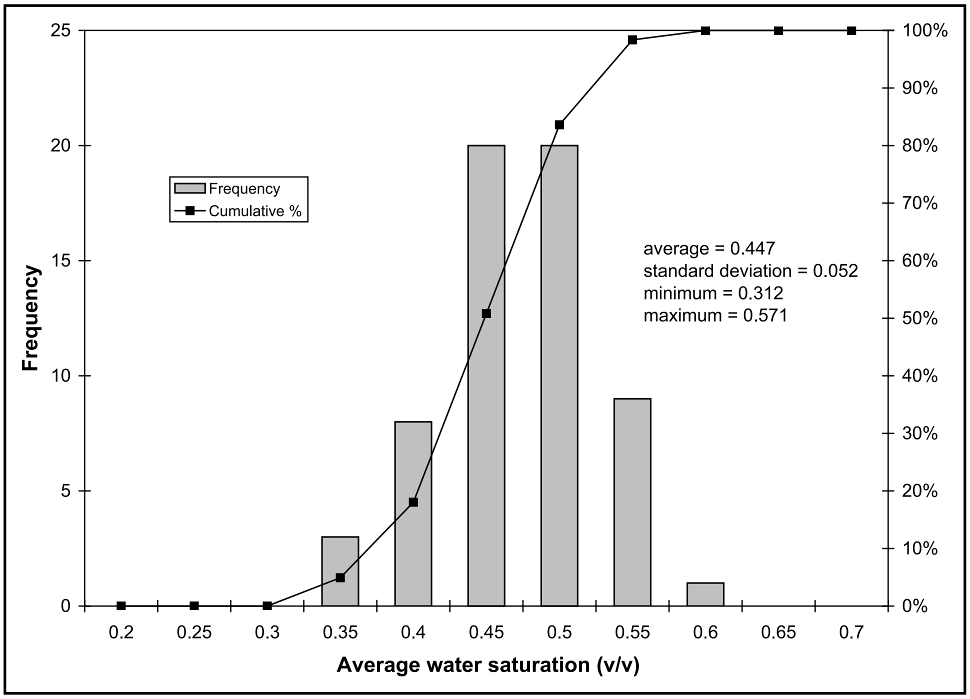


**Figure 17.** Distribution of average water saturation from log analysis, per well, for the upper 2500 ft (760 m) of the Lance Formation. Histogram bars refer to left (frequency) axis; cumulative frequency line (cumulative %) refers to the right axis.

is often poorly characterized. The porosity of tight-gas sandstones is also low, often times below what is considered the lower limit of pay in many other areas. The porosity range illustrated by Figures 9 and 11, for example, is entirely below what is considered net pay in the Tertiary sandstones of the offshore Gulf of Mexico. By Gulf Coast commerciality standards, none of the reservoir rock at Jonah field is net pay. Furthermore, the porosity-permeability relationship in tight-gas sandstones displays a large scatter and also has a strong confining stress

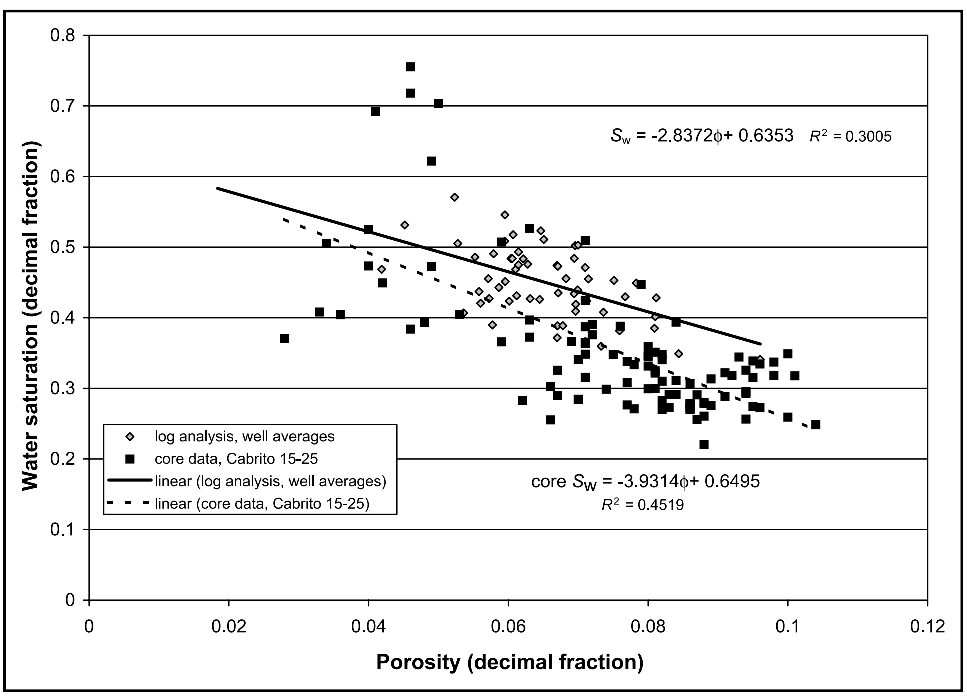


**Figure 18.** Trend of decreasing average water saturation with increasing average porosity in the upper 2500 ft (760 m) of the Lance Formation. Log analysis values and routine core measurements are shown.

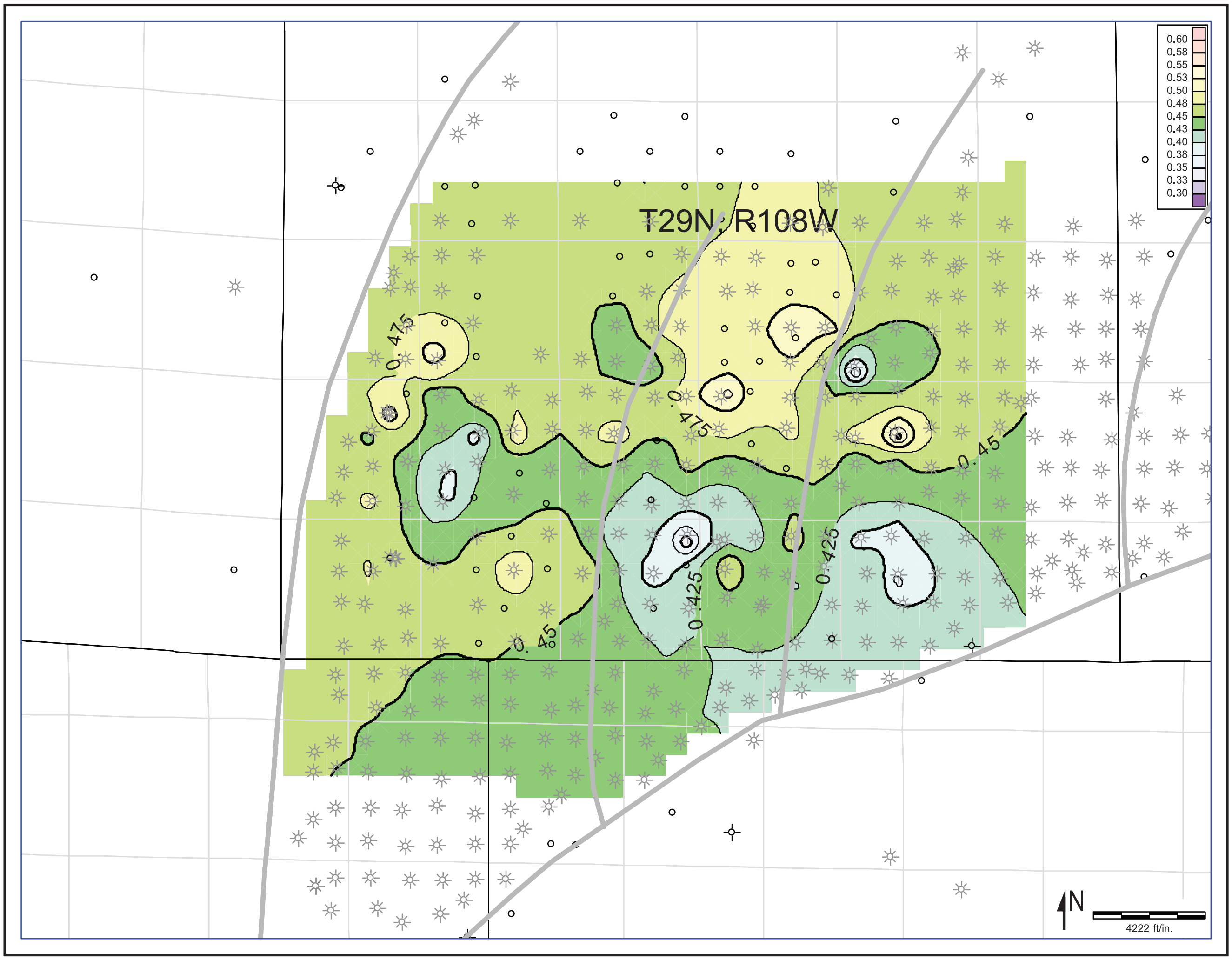


**Figure 19.** Contour map of average water saturation for sandstones in the upper 2500 ft (760 m) of the Lance Formation. Contour interval = 2.5%.

dependence that is not seen in higher permeability reservoir systems. Consequently, it is difficult to pick a porosity value from a porosity-permeability crossplot that correlates to a specific minimum flow criterion. To complicate matters further, tight-gas reservoirs require fracture stimulation that tends to average out differences and makes it difficult to determine which intervals are really flowing gas and at what rates. As fracture stimulation technology improves, tighter and tighter rocks can be stimulated and produced at commercial rates, so net pay criteria tends to shift with time, independent of commodity prices or development costs. Finally, tight-gas reservoirs show a wide spread in calculated water saturations. Fundamental problems in the saturation calculations exist, the most critical being the uncertainty in formation water resistivity. This uncertainty makes it difficult to pick a saturation cutoff that clearly separates wet zones from hydrocarbon-saturated rocks at irreducible water saturation.

Figure 16 illustrates the in-situ (at reservoir stress) relationship between porosity and absolute permeability. Using equation 5.2, we can estimate the average porosity at 1-μd in-situ permeability to be 2.7%. At a permeability of 5 μd, the average porosity is 6.0%. Rocks with less than 5 μd permeability at reservoir conditions produce gas at insignificant rates even after fracture stimulation. The data can also be shown as cumulative flow and cumulative storage plots (Figures 20, 21). Figure 20 shows that more than 90% of the flow capacity of the Lance reservoirs come from rocks with permeability greater than 14 μd. From equation 5.2, this equates to an average

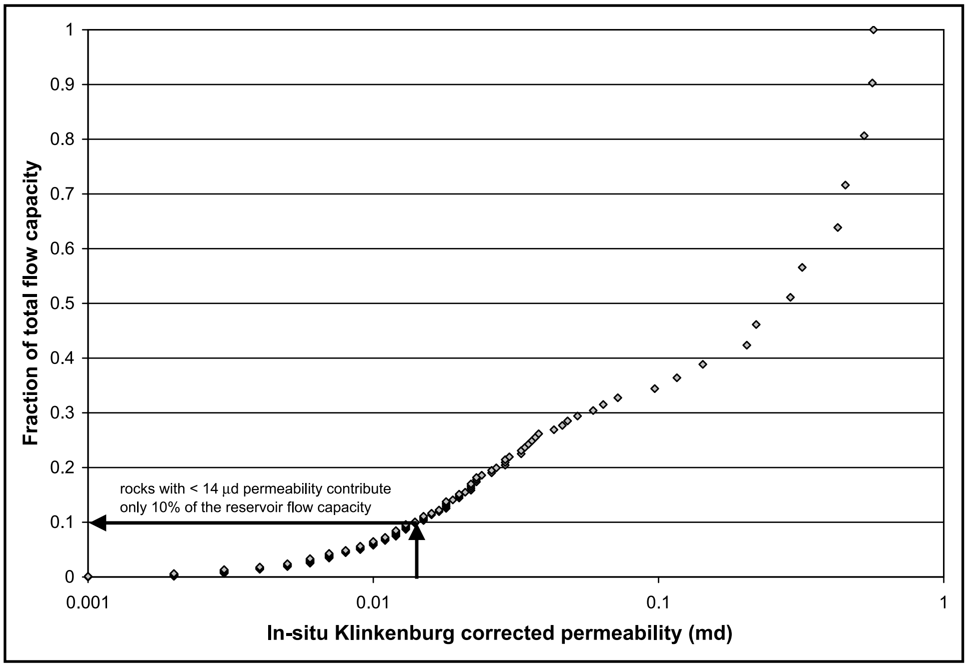


**Figure 20.** Cumulative flow-capacity plot showing fractional flow capacity as a function of in-situ permeability from core data sorted in permeability order.

porosity of 7.8%. Figure 21 illustrates that 38% of the total reservoir storage capacity is in rocks with 7.8% porosity or less. Therefore, although a substantial portion of the reservoir storage is in these low-porosity rocks, they contribute a relatively insignificant part of the total flow capacity.

Figure 22 is a crossplot of cumulative storage versus cumulative flow, sorted in core porosity order. The dramatic break at about 92% cumulative storage represents either a major rock type change to a significantly better porosity-permeability trend or the core plugs that contain microfractures. The top nine samples all have porosity

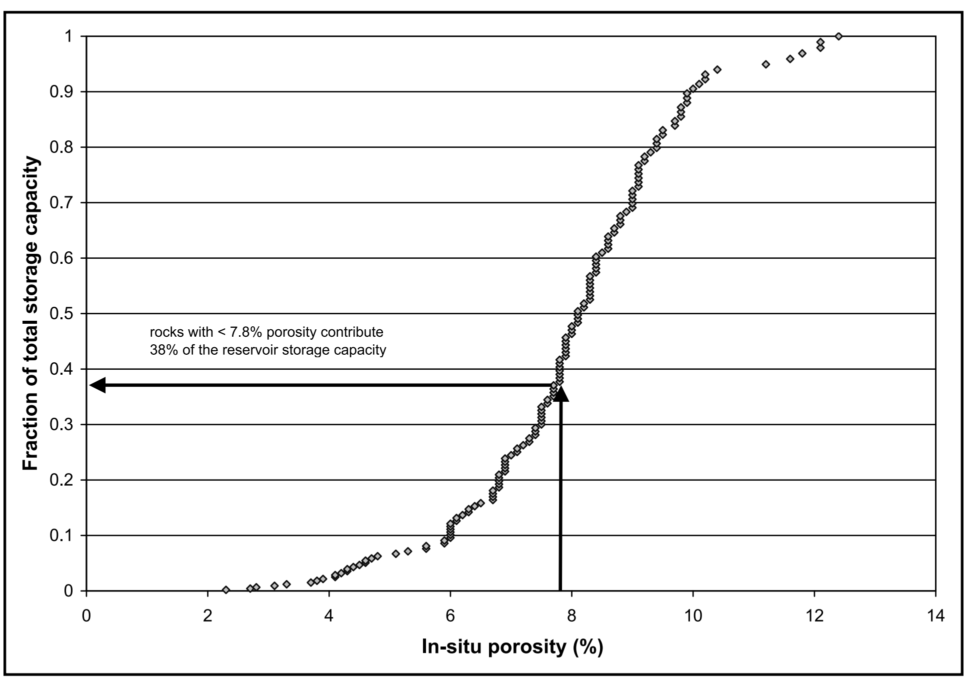


**Figure 21.** Cumulative storage-capacity plot showing fractional storage capacity as a function of in-situ porosity, from core data sorted in porosity order.

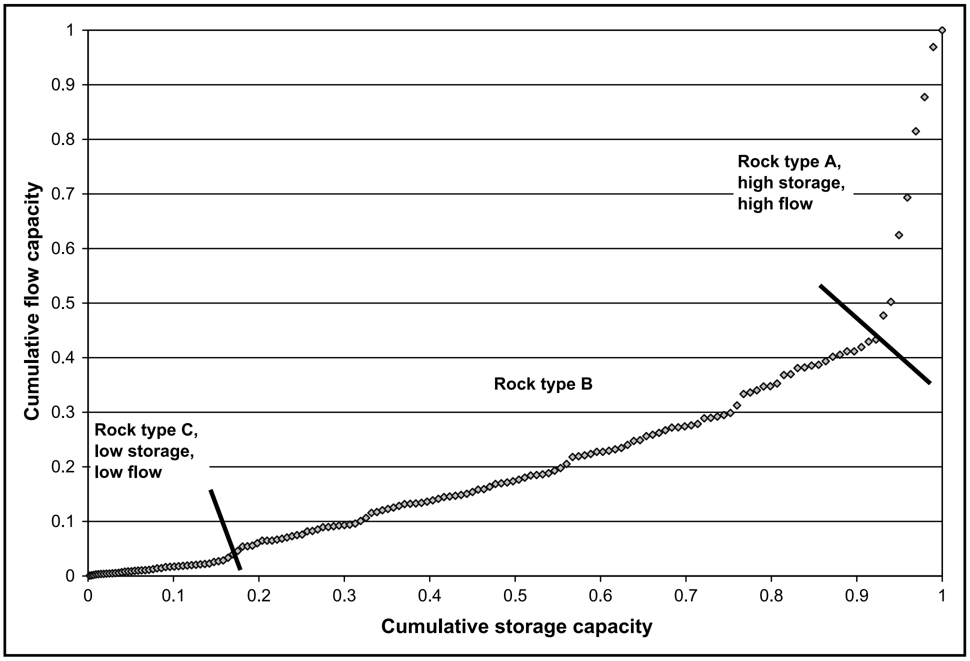


**Figure 22.** Cumulative storage capacity vs. cumulative flow capacity, from core data sorted in ascending porosity order.

in excess of 10.2% (Figures 16, 21). Because the high-permeability samples correlate with high porosities, we suspect that these samples all belong to a distinct, high-quality reservoir rock type (rock type A). Rock type A is so much better than the remainder of the Lance sandstones that they are likely to dominate test results and early production behavior. Based on comparison of the core depths to core descriptions shown by Shanley (2001), most of this rock type consists of trough cross-bedded and convolute-bedded sandstones.

Between 5 and 92% cumulative storage capacity (Figure 21) is a rock type that makes up the bulk of the Lance reservoir (rock type B). Rock type B is predominantly ripple cross-laminated sandstone (Shanley, 2001) but also includes the trough cross-bedded and convolute-bedded facies found in rock type A. More accurate comparisons between petrophysical rock types and core lithofacies will require spotting the precise plug locations on the cores and determining their specific lithotypes.

Rock type C samples have less than 6.7% porosity (Figure 21) and contribute only 5% to the cumulative flow capacity. It is uncertain if these rocks are capable of producing gas, but they would contribute an insignificant portion of the measured flow. If completed and tested in isolation from the better rocks, they would likely produce at noncommercial rates.

This analysis suggests two possible permeability-based pay cutoffs. One cutoff would be equivalent to an average porosity of 6.7% that represents the break between nonreservoir sandstones (rock type C) and the average reservoir rock in the Lance (rock type B). The other cutoff would be equivalent to an average porosity of 10.2%, at the break in slope from the average reservoir rock (rock type B) to the very high-quality reservoir (rock type A) that will dominate the early production behavior. Because this analysis is based on a limited core database in a very large field, and because these are average properties with substantial variance, we used 6 and 10% porosity as cutoffs between nonpay, pay, and high-quality pay.

The determination of cutoffs is actually more complicated because the data in Figure 16 represent dry rock permeability to the gas phase, but in nature, reservoirs contain both water and hydrocarbons. The effective permeability to gas in the presence of water is reduced and is dependent on saturation and the average pore-throat size of the reservoir rocks. Byrnes (1997, his figure 6) illustrates the decrease in effective permeability to gas with increasing water saturation for a large suite of tight-gas sandstones from Rocky Mountain region. Byrnes' (1997) results are generally valid for rocks of similar porosity, permeability, and grain size and are believed to be applicable to the Lance reservoirs at Jonah, although none of the samples in his data set were specifically from this field. Byrnes (1997) found that the relative permeability to gas approaches 100% at irreducible water saturations of approximately 30% or less, and it abruptly decreases to near zero at water saturations above 50–60%.

Table 1

This Table Summarizes the Average Reservoir Properties of All Sandstones in the Lance (Net of the $V_{shale}$ Cutoff Only) Compared to the Net Pay Counts Using All Three Cutoff Values.

| | Gross Thickness (ft) | Net Pay Thickness (ft) | Net/Gross (%) | Net Pay: Average Porosity (%) | Net Pay: Average Storage Capacity (ft) | Net Pay: Average Water Saturation (%) | Net Pay: Average $V_{shale}$ (%) |
|---|---|---|---|---|---|---|---|
| **Net Sand: No $\phi$ or $S_w$ Cutoffs** | | | | | | | |
| Minimum | 2500 | 695 | 28 | 4.2 | 37.9 | 31 | 14 |
| Maximum | 2500 | 1318 | 53 | 9.6 | 102.1 | 57 | 26 |
| Average | 2500 | 991 | 40 | 6.5 | 66.6 | 45 | 17 |
| Standard deviation | | 152 | 6 | 0.9 | 15.4 | 5 | 2 |
| **Net Pay: 6% $\phi$ and 50% $S_w$ Cutoffs** | | | | | | | |
| Minimum | 2500 | 99 | 5 | 7.6 | 8.3 | 20 | 3 |
| Maximum | 2500 | 815 | 39 | 10.9 | 89.2 | 40 | 14 |
| Average | 2500 | 441 | 25 | 9.3 | 41.7 | 33 | 7 |
| Standard deviation | | 133 | 6 | 0.7 | 14.5 | 3 | 2 |
| **Net Pay–Net Sandstone Ratios (%)** | | | | | | | |
| Minimum | | 14 | 18 | 181 | 22 | 64 | 21 |
| Maximum | | 62 | 73 | 114 | 87 | 71 | 54 |
| Average | | 44 | 62 | 144 | 63 | 75 | 43 |

Assuming that the results of our log calculations are valid, and average water saturations in the Lance are 45% (Figure 17), over half of the sandstones will have relative permeabilities to gas of less than 10%. A full net pay cutoff analysis should incorporate relative permeability effects, which should be collected through a large number of single end-point effective permeability measurements on core. Because these data are not available, the impact of relative permeability is incorporated through a water saturation cutoff. A 50% water saturation cutoff is used as a hard net pay cutoff because the data of Byrnes (1997) indicate insignificant relative permeability to gas at higher saturations. Most sandstones with less than 6% porosity display high average water saturation (Figure 18), which reinforces the use of a 6% cutoff.

Finally, we used a 50% $V_{shale}$ cutoff to cleanly separate the reservoir sandstones from shaly nonreservoir rocks. Interestingly, the net pay counts are not highly sensitive to the exact value used because nearly all sandstones with porosity greater than 6% are significantly cleaner than this cutoff. Some shaly siltstones with porosity in the 6–8% range may be cut out using this criterion. We have observed considerable variation in net pay counts when using an uncorrected gamma-ray cutoff, which serves to emphasize the importance of careful log normalization.

## Net Pay Summations

Reservoir properties were summed over the top 2500 ft (760 m) of the Lance using the following three petrophysical cutoffs: (1) 50% $V_{shale}$ cutoff; (2) 6% density-neutron effective porosity cutoff; and (3) 50% $S_w$ cutoff.

Table 1 summarizes the average reservoir properties of all sandstones in the Lance (net of the $V_{shale}$ cutoff only) compared to the net pay counts using all three cutoff values. Alternative cases were run using 4, 8, 10, and 12% effective porosity cutoffs. The latter two cases result in uncomfortably low net pay counts but are useful for mapping intervals of very high-quality pay. The net 8% case is relatively uninteresting, because it is only slightly different than the net 6% case and, based on Figure 21, is an arbitrary cut in the dominant rock type in this reservoir system.

Based on the defined cutoffs, the net pay thickness is 14–62% (average 44%) of the net sandstone counts

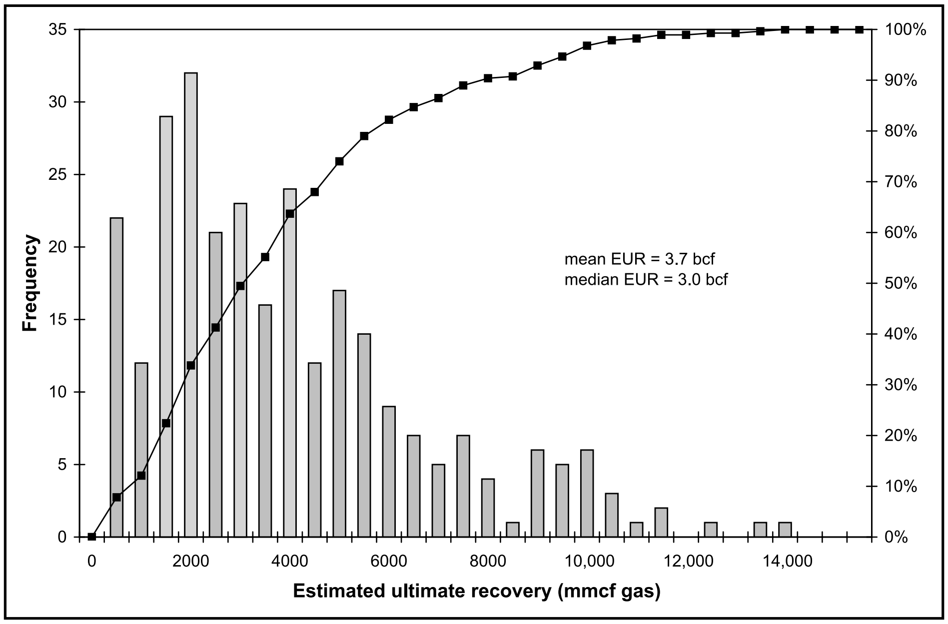


**Figure 23.** Distribution of estimated ultimate recoveries, in million cubic feet of gas, from decline curve analysis. Histogram bars refer to left (frequency) axis; cumulative frequency line (cumulative %) refers to the right axis.

discussed above. The average net pay thickness is 441 ft (134 m), compared to an average net sandstone thickness of almost 1000 ft (300 m). Obviously, a large portion of the sandstones passing a 50% $V_{\text{shale}}$ cutoff are low porosity, as shown in Figures 11, 13, and 20. In particular, note the secondary low-porosity peak in Figure 13, which represents a distinct rock type of very fine-grained sandstones and siltstones with less than 10 μd in-situ permeability, which is probably not part of the productive reservoir system.

The average porosity of net pay is greater than the average porosity of all sandstones, because the low-porosity tail has been cut off. The average net pay porosity by well ranges from 7.6 to 10.9% and averages 9.3% (Table 1). Similarly, the water saturation of net pay is lower, because the high water saturation and low-porosity sandstones have been cut out, resulting in an average water saturation for net pay of 33%, as compared to 45% for all sandstones. Average water saturations are as low as 20% in a few wells.

## Estimated Ultimate Recovery

The distribution of EURs based on decline curve analysis is shown in Figure 23. The mean EUR is 3.7 bcf gas, with a range from 0 to 13.7 bcf gas. The EUR distribution is log normal, so the median reserves are slightly lower at 3.0 bcf. About 20% of the wells will make more than 6 bcf gas, which is one reason why Jonah is considered such an outstanding field. The initial decline rates range from 30 to 100% per year and average 70% (Figure 24). Many Jonah wells have been recompleted during their productive life, so the initial production rate ($Q_i$) (in million cubic feet per month) from the decline analysis is for the most recent production history. As a result, $Q_i$ correlates poorly with EUR. Initial production ranges from 1 to 323 mmcf/month and averages 108 mmcf/month (Figure 25).

Figure 26 is a map of EUR across Jonah field and shows the location of the major known faults (Montgomery and Robinson, 1997). The most striking feature of this map is the increased density of high-EUR wells against the updip portion of each fault block. The pattern suggests that the faults are sealing faults, and gas was structurally trapped into several pools as it migrated updip into the field area.

## Net Hydrocarbon Pore Volume versus Estimated Ultimate Recovery

Net hydrocarbon pore volume was calculated from the net pay summations using a fieldwide average gas-formation volume factor. A crossplot of the calculated net feet of hydrocarbon in place versus EUR is shown in Figure 27. The regression line through the dominant cloud of points is

$$\text{EUR (mmcf gas)} = 108 \times \text{NHPV} - 873, \quad r^2 = 0.795 \tag{6}$$

where NHPV is the net hydrocarbon pore volume in feet ($Sg \times \Phi \times H$; all net of 50% $V_{\text{shale}}$, 50% $S_w$, and 6%

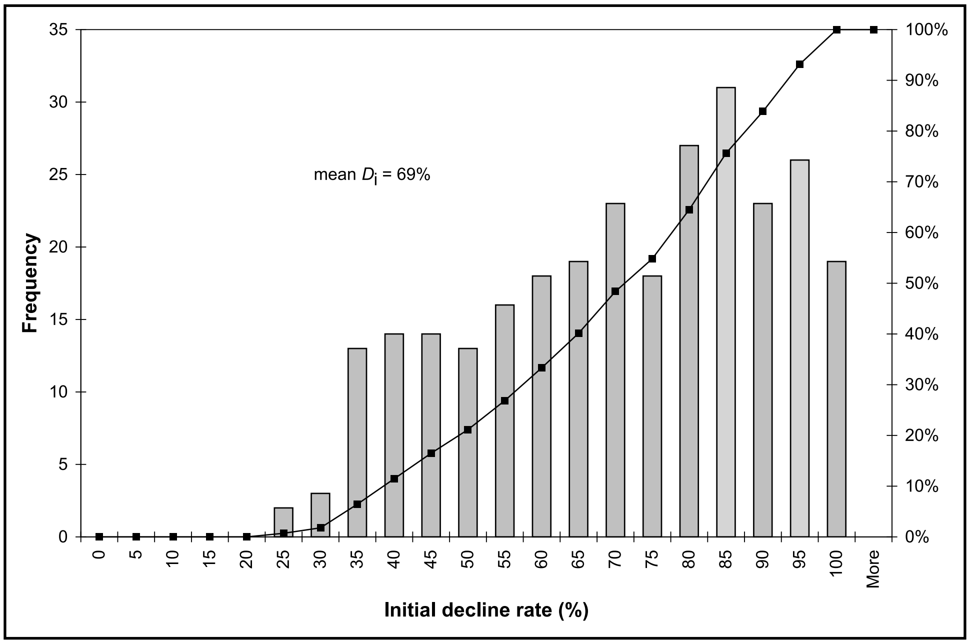


**Figure 24.** Distribution of initial decline rates, in %, from decline curve analysis. Histogram bars refer to left (frequency) axis; cumulative frequency line (cumulative %) refers to the right axis.

porosity cutoffs). Using the field average of 440 ft (130 m) of net pay, 9.3% porosity, and 33% water saturation, an average well will have 31.5 ft (9.6 m) net of hydrocarbon pore volume. Based on equation 6, the expected EUR is 2.5 bcf gas per well, which is close to the median reserves but is significantly less than the actual field average of 3.9 bcf gas. This difference is caused by the log-normal distribution, wherein the average is skewed toward the large wells on the high tail of the distribution (Figure 20).

The regression line in Figure 27 was determined by excluding two clouds of outliers, one representing wells that are significantly "overproducing" and another smaller group that is "underproducing." To determine if the outliers are random error, completion related, or geologically

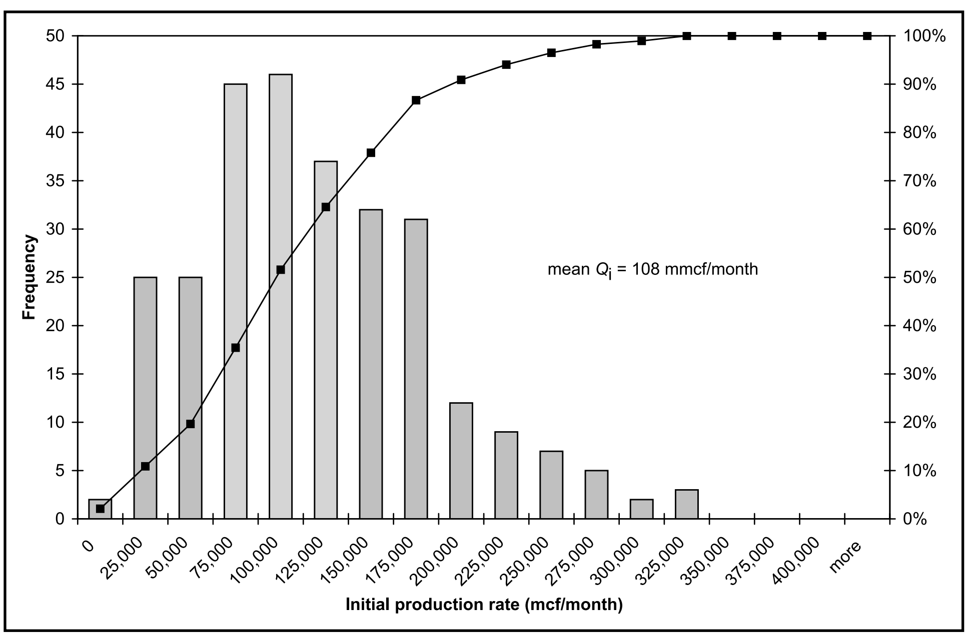


**Figure 25.** Distribution of average initial producing rates, in thousand cubic feet per month, from decline curve analysis. Histogram bars refer to left (frequency) axis; cumulative frequency line (cumulative %) refers to the right axis.

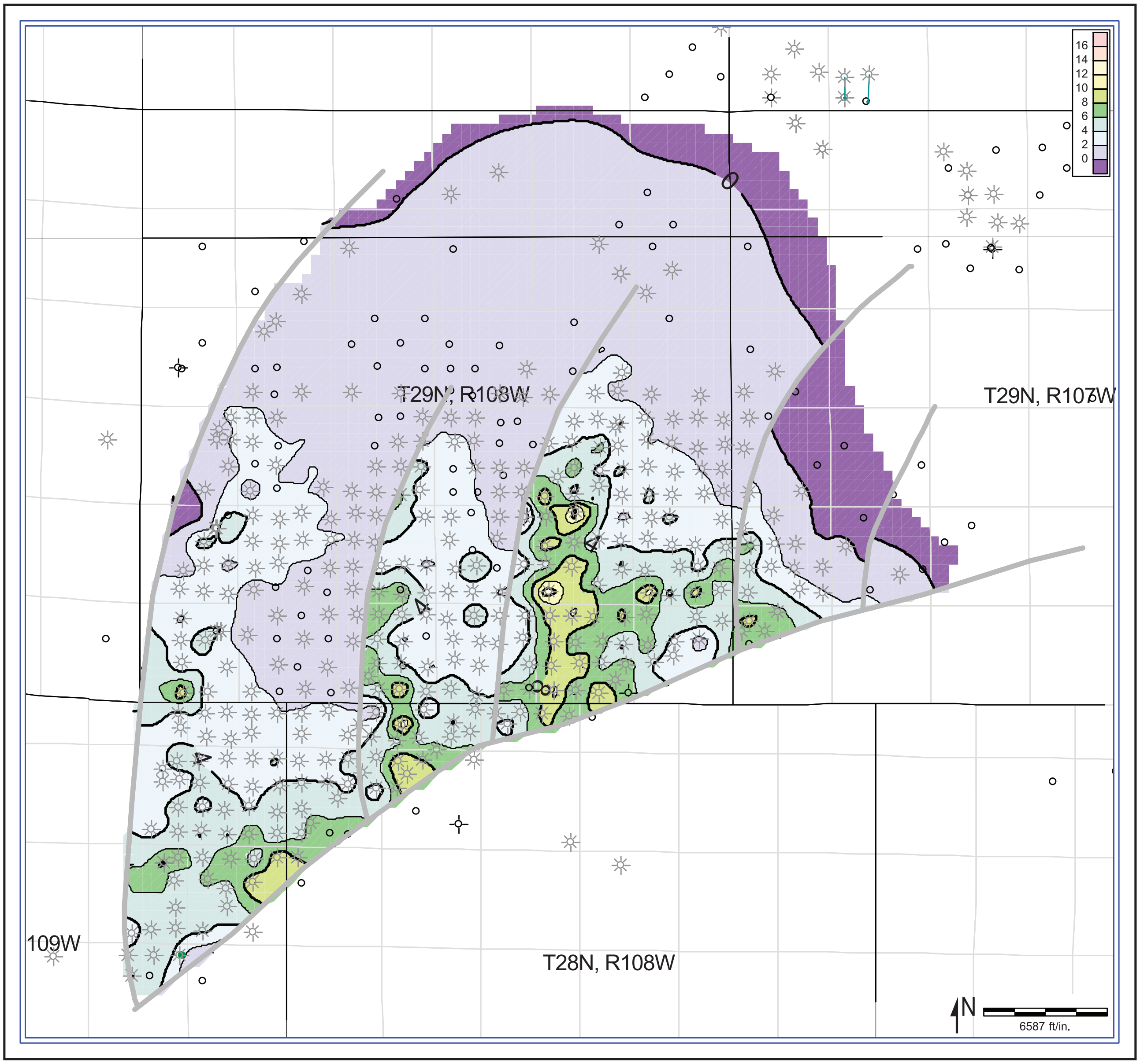


**Figure 26.** Estimated ultimate recovery (in bcf gas) from decline curve analysis for wells in Jonah field. Contour interval = 2.0 bcf gas.

controlled, we calculated and mapped the difference between the predicted EUR and actual EUR for all wells in the study area (Figure 28). The overproducers are clustered on the east side of the large intrafield faults, whereas the underproducers are on the west side of those faults. This pattern mimics the overall EUR pattern shown in Figure 26.

The hydrocarbon pore volume in the underproducers and the overproducers overlap, indicating that the differences across the faults are not simply caused by a greater amount of gas-charged sandstone on one side when compared to the other. The dramatic differences in productivity are entirely related to permeability and, more specifically, to relative permeability effects, instead of bulk formation permeability. Because of the steepness of the relative permeability curves in tight-gas sandstones, very small differences in saturation can have a significant impact on the recovery efficiency from the pore system. The overproducers represent high average recovery efficiency (high relative permeability to gas), whereas the underproducers represent low recovery efficiency (low relative permeability to gas). Better production in the

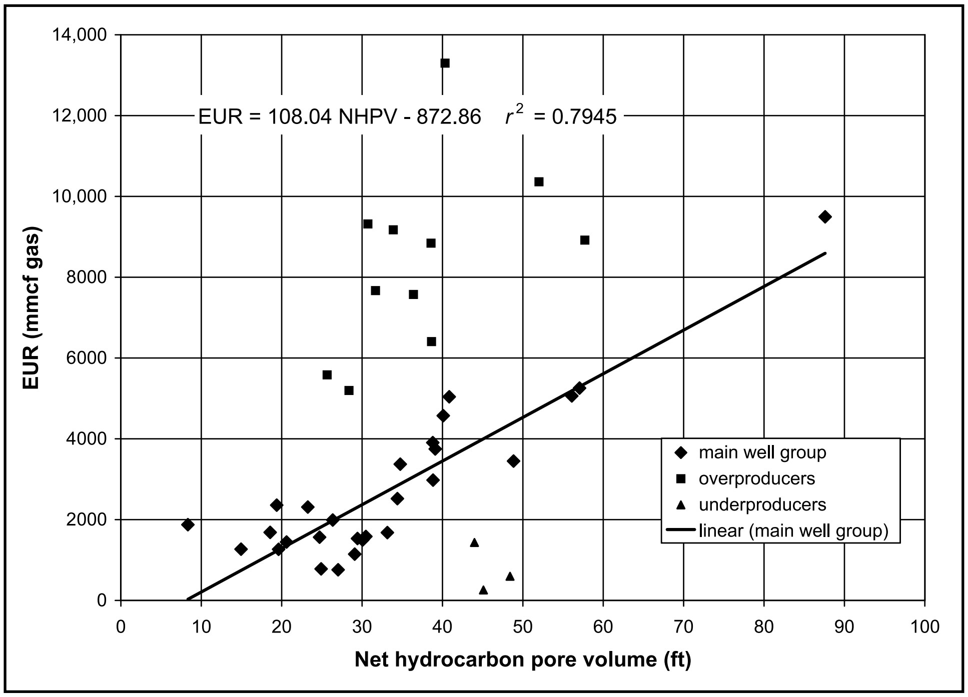


**Figure 27.** Net hydrocarbon pore volume in the upper 2500 ft (760 m) of the Lance Formation compared to estimated ultimate recovery (mmcf gas) from decline curve analysis.

updip regions of each fault block can be explained by the effectiveness of the sealing fault and minor changes in the water saturation from the downdip to updip portions of each fault block. The errors associated with log-derived water saturations are fairly large; a 10% change in water saturation across a fault boundary might not be detectable but could have a two to five times greater impact on recovery.

The effect of relative permeability on both gas production and water cut is dramatically illustrated by the producing water-gas ratios (WGR) of the wells at Jonah (Figure 29). The WGR at Jonah ranges from 0.1 to 70 bbl/mmcf gas, with 93% of the wells producing less than 12 bbl/mmcf gas. Until recently, it was thought that the field was making little, if any, formation water, because the average WGR for the field is a relatively insignificant 3.1 bbl/mmcf gas. Mapping revealed a smooth increase in WGR downdip across the field, with very low values (<1.0 bbl/mmcf gas) in the highest structural positions in each separate fault block. The water of condensation based on dew-point calculations should be on the order of 1 bbl/mmcf gas, so the updip wells appear to be producing dry gas free of any formation water. These wells must be near irreducible water saturation and at or below critical water saturation.

The downdip wells at Jonah are making relatively small water cuts, but the large cumulative production acts as an amplifier to reveal even small differences in relative permeability to water. As water saturation increases, the relative permeability to water also increases, and consequently, the produced WGR increases. As the relative permeability to gas decreases, the gas rates decline, and total productivity is diminished. Thus, Figures 26 and 29 are almost identical, even in their fine details, with the wells with low EURs also having significantly higher WGRs. Outside the two major bounding faults and along the downdip northeast edge of the field, the wells are producing greater than 20 bbl water/mmcf gas, and EURs are 1.0 bcf gas or less. These wells still have some relative permeability to gas, at least in the best sandstones that were perforated, and are therefore above critical gas saturation. The total spread of water saturation from the best wells in the updip areas of each fault block to the downdip limits is estimated to be 20–30%, based on our log calculations and core analysis (Figures 17, 18).

## CONCLUSIONS

The upper 2500 ft (760 m) of the Lance Formation at Jonah field averages 40% net sandstone, half of which has porosity greater than 6% and is considered potential pay on the basis of porosity-permeability relationships. As a result, each well has an average of about 500 ft (150 m) of reservoir sandstone in a typical 2500-ft (760-m) section drilled. The average porosity for all sandstones at

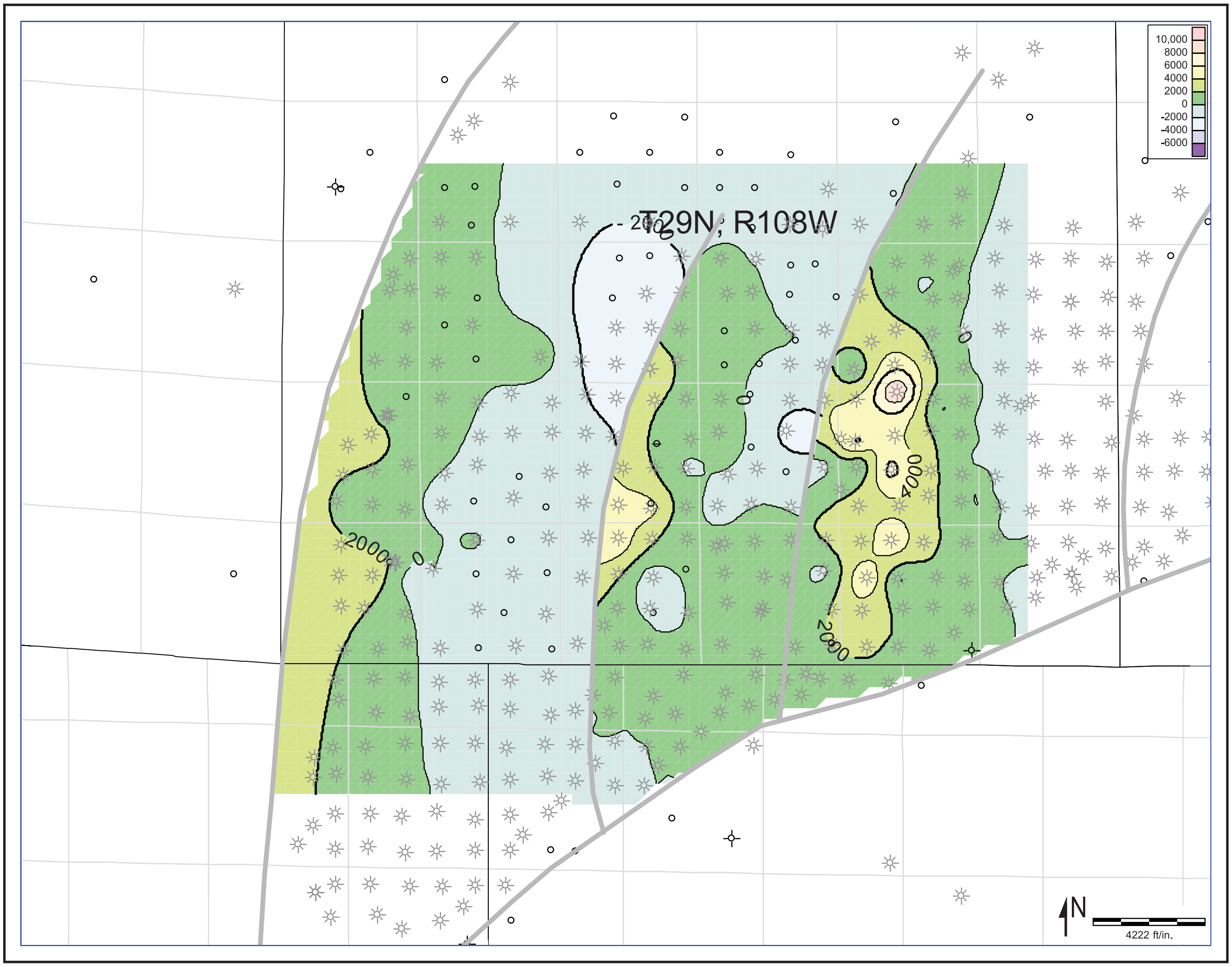


**Figure 28.** Map showing residual values between regression predicted EUR and actual EUR from decline curve analysis (mmcf gas). Contour interval = 2000 mmcf gas (2 bcf gas).

Jonah is 6.5% for log data and 7.1% for core data. As a subset of the sandstones meeting the 6% porosity cutoff, the average porosity of the reservoir-quality sandstones is 9.3%.

The permeability of these sandstones ranges from 1 μd to a few hundreds of microdarcys. The average in-situ reservoir permeability at the average log porosity of 6.5% is only 6 μd, whereas for the average porosity of net pay (9.3%), the average permeability improves to 25 μd. This latter value compares favorably with unpublished estimates of the average reservoir permeability from single-well modeling.

Water saturations averaged over the entire Lance range from 30 to 60%. Water saturation correlates with porosity and permeability. Higher water saturation values are associated with the lower porosity, nonreservoir rocks. Reservoir-quality sandstones have water saturations from 20 to 40% and average 33% for all wells. Subtle differences in water saturation resulting from rock-quality changes can have a dramatic impact on the effective permeability to gas because of steep relative permeability curves.

The EURs of the 40-ac (0.16-km$^2$) spacing wells at Jonah field range from 0 to almost 14 bcf gas, with an average of a little less than 4 bcf. Given the very low average porosity and permeability of the reservoir sandstones, it is perhaps surprising that these wells can produce gas

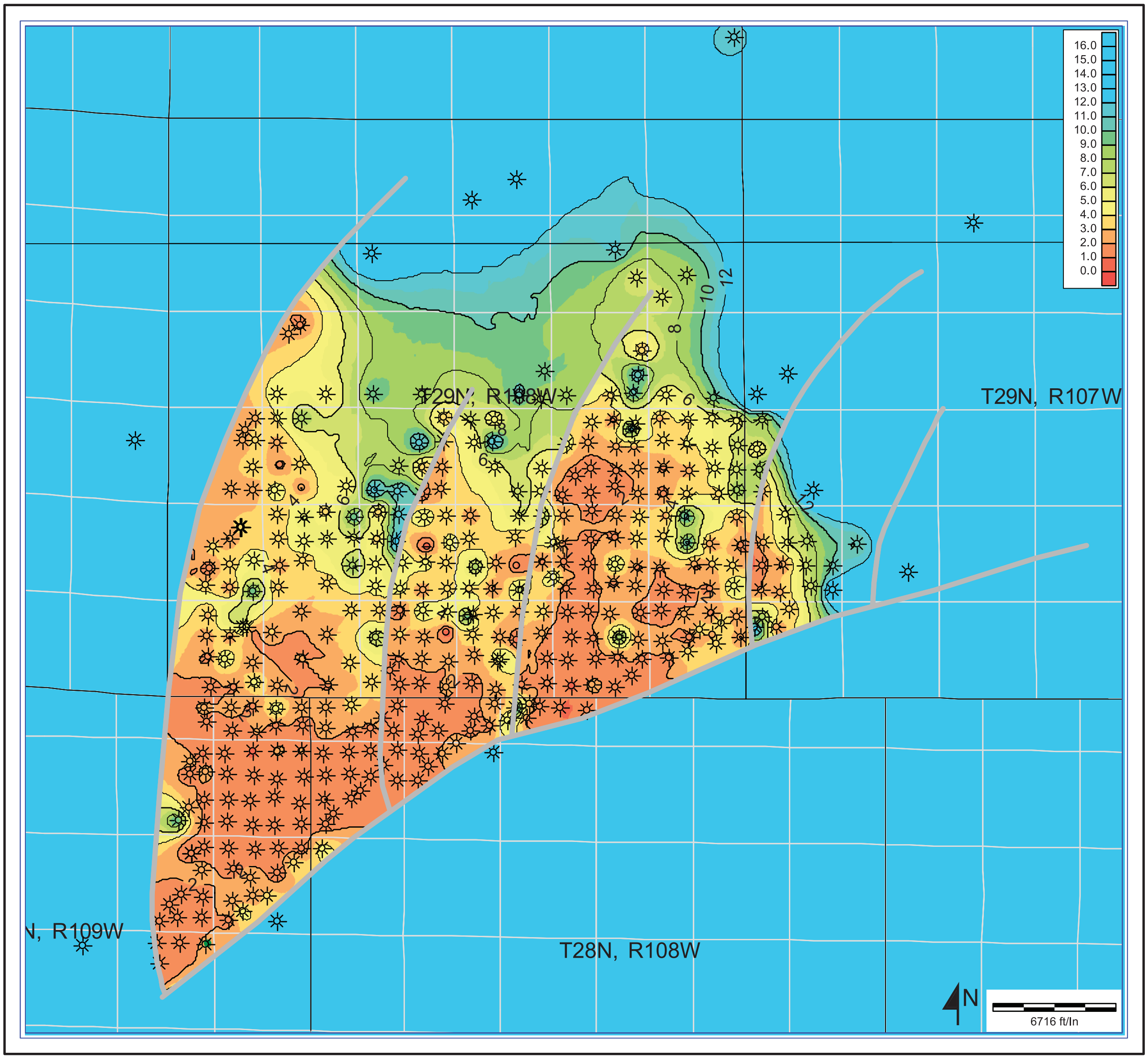


**Figure 29.** A Map illustrating producing water-gas ratios across Jonah Field. The water-gas ratio ranges from 0.1 bbl water/mmcf in structurally high positions of the field to 70 bbl water/mmcf in downdip portions. Contour interval is in barrels of water per million cubic feet of gas.

at all. In most sandstone reservoirs around the world, the entire Lance section at Jonah would be considered a nonreservoir rock and below the net pay cutoffs for gas production.

What separates Jonah from other fields in the Rocky Mountain region are the substantial net pay thickness of low-permeability gas sandstone in the Lance Formation and the large areal extent of the field. The application of effective stimulation methods to complete multiple-pay sandstones over the thick interval yields a world-class giant gas field in reservoirs having permeabilities in microdarcys.

## REFERENCES CITED

Asquith, G. B., 1990, Log evaluation of shaly sandstones: A practical guide: AAPG Continuing Education Course Notes Series 31, 59 p.

Bowker, K. A., 1995, Lance and Mesaverde of the Hoback basin:

Preliminary results from recent drilling, *in* Geological characterization of the cretaceous gas plays in the Greater Green River basin: Gas Research Institute/Department of Energy/Independent Petroleum Association of Mountain States Greater Green River Consortium Symposium, p. 280–296.

Bowker, K. A., and J. W. Robinson, 1997, Jonah field: A shallow sweetspot in the basin-centered gas accumulation of the northern Green River basin, Wyoming: AAPG Bulletin, v. 81, p. 1219, and Expanded Abstracts Volume, p. 25–30.

Byrnes, A. P., 1997, Reservoir characteristics of low-permeability sandstones in the Rocky Mountains: The Mountain Geologist, v. 34, p. 39–48.

Clavier, C., G. Coates, and J. Dumanoir, 1977, The theoretical and experimental bases for the "dual water" model for the interpretation of shaly sands: Society of Petroleum Engineers Paper 6859, 16 p.

Cluff, R. M., 2004, Production history plots for Jonah field, Sublette County, Wyoming, *in* J. W. Robinson and K. W. Shanley, eds., Jonah field: Case study of a tight-gas fluvial reservoir: AAPG Studies in Geology 52, CD-ROM, Appendix C.

Cluff, R. M., and C. M. Murphy, 2004, Stratigraphic cross sections through Jonah field, Sublette County, Wyoming, *in* J. W. Robinson and K. W. Shanley, eds., Jonah field: Case study of a tight-gas fluvial reservoir: AAPG Studies in Geology 52, CD-ROM, Appendix B.

Dewan, J. T., 1983, Essentials of modern open-hole log interpretation: Tulsa, PennWell Books, 361 p.

DuBois, D. P., P. J. Wynne, T. M. Smagala, J. L. Johnson, K. D. Engler, and B. C. McBride, 2004, Geology of Jonah field, Sublette County, Wyoming, *in* J. W. Robinson and K. W. Shanley, eds., Jonah field: Case study of a tight-gas fluvial reservoir: AAPG Studies in Geology 52, p. 37–60.

Eberhard, M., and M. Mullen, 2001, The effect of stimulation methodologies on production in the Jonah field: Rocky Mountain Petroleum Technology Conference, Society of Petroleum Engineers, Keystone, 21–23 May 2001, SPE paper 71048, 9 p.

Hook, J. R., 2003, An introduction to porosity: Petrophysics, v. 44, no. 3, p. 205–212.

Montgomery, S., and J. W. Robinson, 1997, Jonah field, Sublette County, Wyoming: Gas production from overpressured Upper Cretaceous Lance sandstones of the Green River basin: AAPG Bulletin, v. 81, p. 1049–1063.

Shanley, K. W., 2001, Fluvial reservoir description for a tight-gas giant: Jonah field, Green River basin, Wyoming, *in* J. W. Robinson and K. W. Shanley, eds., Tight-gas fluvial reservoirs: A case history from the Lance Formation, Green River basin, Wyoming: AAPG Annual Convention, Denver, Colorado, AAPG Short Course 2, 49 p.